Table of Contents:

---

1. General

^{1}H and ^{13}C NMR spectra were recorded at room temperature on a JEOL JNM-ECS-400 NMR spectrometer at 400 and 100 MHz, respectively. The proton chemical shift values are reported in parts per million (ppm) downfield from tetramethylsilane and referenced to the proton resonance of $CHCl_3$ (δ7.26), CD_3OD (δ3.31), D_2O (δ4.79) or ^{t}BuOH (δ1.23). The carbon chemical shift values are reported in parts per million (ppm) downfield from tetramethylsilane and referenced to the carbon resonance of $CDCl_3$ (δ 77.0), CD_3OD (δ49.0) or THF-d_8 (δ67.2). Chemical shifts are reported in ppm and *J* values in Hz. The data are presented in the following order: chemical shift, signal area integration in natural numbers, multiplicity (s = singlet, d = doublet, t = triplet, q = quartet, quint = quintet, m = multiplet and/or multiple resonances, and br = broad) and coupling constant. ESI-MS spectra were measured on a Bruker micrOTOF-QII-RSL. Anhydrous methanol (MeOH), dichloromethane (CH_2Cl_2) and tetrahydrofuran (THF) were purchased from Kanto. Other solvents used were purchased from Wako Pure Chemical Industries, Ltd. (Wako) or Tokyo Chemical Industry Co. Ltd. (TCI), and were used as received. Reactions conducted below room temperature were cooled using a PSL-1400 (Tokyo Rikakikai Co., Ltd.) or a PSL-1810 (Eyela). Analytical thin-layer chromatography (TLC) was performed on Silica gel 60 F254-coated glass plates (Merck); visualization of the developed chromatogram was performed by ultraviolet illumination (254 nm) and/or staining with cerium molybdate stain (Hanessian's stain). Flash

column chromatography was performed using silica gel 60N (40-50 μm, Kanto Chemical Co., Inc.) and CHROMATOREX® NH (NH–DM1020, 100–200 mesh, Fuji Silysia Chemical, Ltd.). Gel permeation chromatography (GPC) was performed using a Recycling Preparative HPLC LC-918 (Japan Analytical Industry Co., Ltd.) equipped with two polystyrene columns (YMC-GPC T2000 and YMC-GPC T4000). Reversed-phase HPLC experiments were conducted using an LC-20AP pump, equipped with SPD-M20A detector and CTO-20AC column oven (Shimadzu). Freeze-drying was performed using a freeze dryer (FDU-1200, Eyela) equipped with a Chemistry-HYBRID pump RC 6 (Eyela) for thermally unstable compounds. A MI129 pH ISFET Portable Meter (Mettler Toledo) was used to measure pH.

2. Synthesis of epidithiodiketopiperazines 4 and 5

The previously developed synthetic route to (±)-PS-ETP-1 (**3**), [S1] whose structure is shown in Fig.2 in the main text, has two problems for the synthesis of optically active ETPs. First, introduction of the sulfur functionality into the diketopiperazine (DKP) unit required multiple steps, including radical bromination, removal of overreacted bromine by reduction, hydrolysis, and substitution with toxic H_2S gas, to avoid elimination of the hydroxyl group upon enolate formation. Second, racemization occurred even if optically pure DKP was used. To circumvent these problems, we used the DKP **8** as an intermediate, which can be constructed from alanine and hydroxyproline derivatives, instead of the ETP starting from serine and proline derivatives that we used previously.[S1] The diketopiperazine **8** was synthesized according to the previously reported procedure (Scheme S1).[S1-S3] The procedures described here were not optimized.

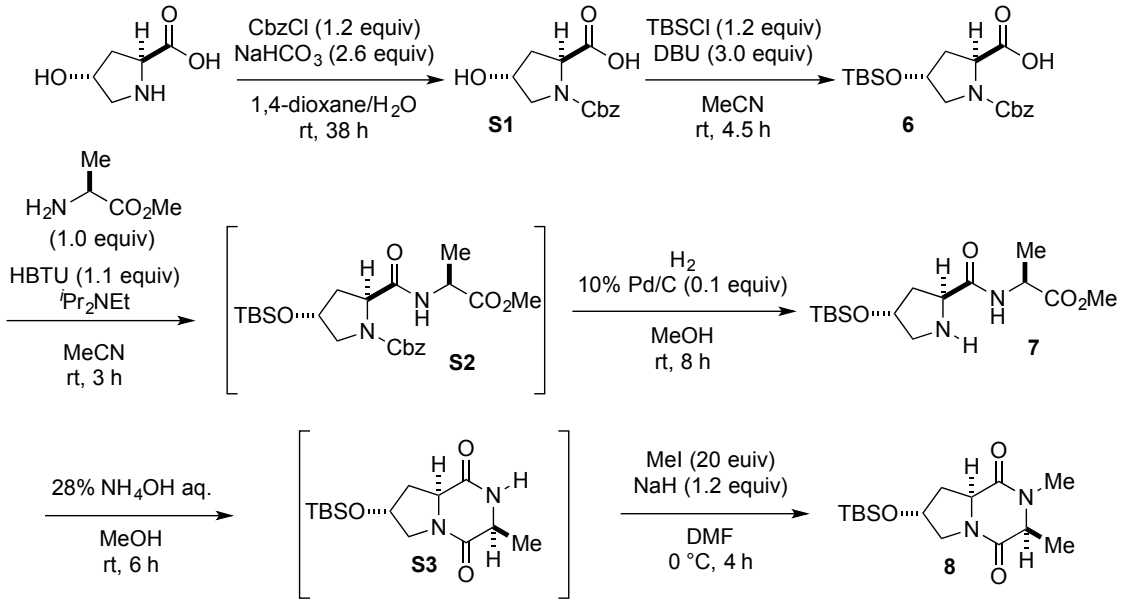

Scheme S1. Synthesis of diketopiperazine **8.**

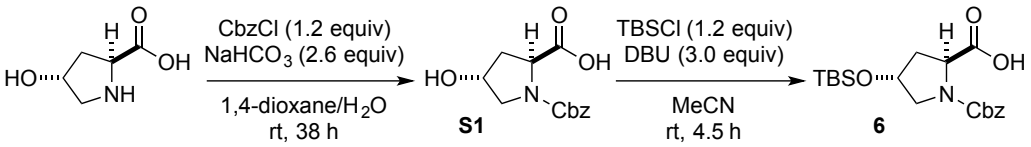

A solution of benzyl chloroformate (1.33 mL, 9.33 mmol) in 1,4-dioxane (2.59 mL) was added dropwise to a stirred solution of *trans*-4-hydroxy-L-proline (1.02 g, 7.78 mmol) and sodium hydrogen carbonate (1.70 g, 20.2 mmol) in water (7.78 mL) at room temperature. The reaction mixture was stirred for 38 h, then diethyl ether (20 mL) was poured into it at room temperature. The aqueous layer was washed with diethyl ether (20 mL × 2), and acidified with hydrochloric acid to pH 2. The resulting mixture was extracted with ethyl acetate (20 mL × 3). The combined organic layer was dried over anhydrous sodium sulfate and evaporated to afford the crude carboxylic acid intermediate **S1**, which was used for the next reaction without purification. To a solution of the crude **S1** and DBU (3.56 mL, 23.3 mmol) in acetonitrile (19.4 mL, 0.4 M) was added *tert*-butyldimethylsilyl chloride (1.41 g, 9.32 mmol) under a nitrogen atmosphere. The reaction mixture was stirred at room temperature for 4.5 h at room temperature, and concentrated *in vacuo*. The residue was purified by silica gel column chromatography (chloroform/methanol = 100/0 to 95/5 to 90/10) to give **6** (1.52 g, 2 steps 52%, as a colorless oil). The NMR spectra for **6** were identical with reported data.[S4]

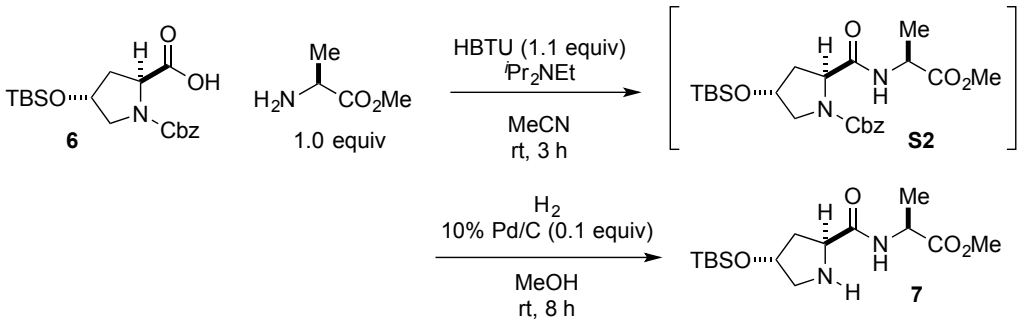

To a solution of **6** (605 mg, 1.59 mmol), L-alanine methyl ester (222 mg, 1.59 mmol) and HBTU [*N,N,N′,N′*-tetramethyl-*O*-(benzotriazol-1-yl)uranium: 665 mg, 1.75 mmol] in acetonitrile (5.3 mL, 0.3 M) was added $^{i}Pr_2NEt$ (333 μL, 1.91 mmol). The reaction mixture was stirred for 3 h at room temperature, and then water (10 mL) was added to it. The aqueous layer was extracted with ethyl acetate (20 mL × 3). The organic layer was washed with hydrochloric acid (2 M, 60 mL), water (60 mL), 2.5% sodium hydrogen carbonate (60 mL), water (60 mL) and brine (60 mL), and dried over anhydrous sodium sulfate. After removal of the solvent, the resulting crude **S2** was used for the next reaction without purification.

To a solution of the crude **S2** in methanol (15.6 mL, 0.1 M) was added 10% Pd/C (166 mg, 10 mol% Pd). The reaction mixture was stirred under a hydrogen atmosphere (balloon) for 8 h, then diluted with ethyl acetate, and passed through Celite® to remove Pd/C. The eluate was evaporated and the residue was washed with ethyl acetate, dried under reduced pressure, and purified by flash column chromatography (chloroform) to give the corresponding *sec*-amine **7** (396 mg, 2 steps 75%, as a colorless oil).

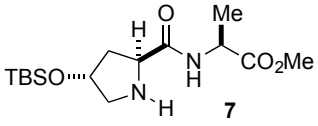

7

^{1}H NMR (400 MHz, $CDCl_3$) δ 7.85 (br s, 1H), 4.68-4.61 (br, 1H), 4.53-4.45 (m, 1H), 3.73 (s, 3H), 3.39-3.31 (br, 1H), 3.26–3.19 (br, 1H), 2.43–2.36 (br, 1H), 2.19-2.12 (br, 1H), 1.46 (d, J = 7.4 Hz, 3H), 0.88 (s, 9H), 0.09 (s, 3H), 0.08 (s, 3H); **^{13}C NMR** (100 MHz, $CDCl_3$) δ 172.8, 169.9, 71.2, 58.9, 54.0, 52.4, 48.5, 39.2, 25.6, 17.9, 17.3, –4.9, –5.0.

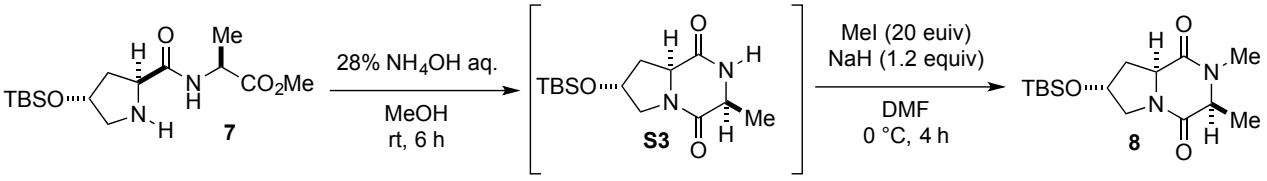

To a solution of **7** (255 mg, 771 μmol) in methanol (48.3 mL, 15 mM) was added 28% aqueous NH_4OH solution (3.1 mL). The reaction mixture was stirred for 6 h at room temperature, then concentrated *in vacuo*, and the residue was roughly purified by flash column chromatography (chloroform/methanol = 100/0 to 98/2) to give the corresponding diketopiperazine **S3** (225 mg). To a solution of **S3** (225 mg, 754 μmol) and methyl iodide (940 μL, 15.1 mmol) in *N*,*N*-dimethylformamide (7.5 mL, 0.1 M) was added sodium hydride (48.3 mg, 905 μmol) at 0 °C under a nitrogen atmosphere. The reaction mixture was stirred at 0 °C for 4 h under a nitrogen atmosphere and for 1 h at room temperature, and then saturated NH_4Cl aq (5 mL) was added to it. The aqueous layer was extracted with ethyl acetate (10 mL × 3). The organic layer was dried over anhydrous sodium sulfate and concentrated in vacuo. The residue was purified by flash column chromatography (chloroform) to give **8** (245 mg, 99%, as a colorless amorphous solid).

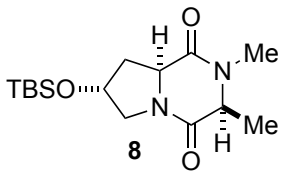

8

^{1}H NMR (400 MHz, $CDCl_3$) δ 4.45 (t, J = 4.4 Hz, 1H), 4.40 (dd, J = 11.0, 6.0, Hz, 1H), 4.13 (q, J = 6.9 Hz, 1H), 3.75 (dd, J = 12.6, 4.4 Hz, 1H), 3.44 (d, J = 12.4 Hz, 1H), 3.00 (s, 3H), 2.35 (dd, J = 13.0, 6.2 Hz, 1H), 2.06 (ddd, J = 12.9, 10.8, 4.1 Hz, 1H), 1.59 (d, J = 6.9 Hz, 1H), 0.87 (s, 9H), 0.09 (s, 3H), 0.08 (s, 3H); **^{13}C NMR** (100 MHz, $CDCl_3$) δ 168.8, 165.5, 68.8, 57.3, 56.2, 55.1, 39.1, 30.0, 25.7, 18.0, 15.2, –4.8, –5.0; **$[\alpha]_D^{28}$** –65 (*c* 1.0, $CHCl_3$); **FTIR** (neat) 3002, 2954, 2931, 2886, 2858, 1665, 1459 cm^{-1}; **HRMS-ESI**

calcd for $C_{15}H_{29}N_2O_3Si$ $[M+H]^+$: 313.1947, found: 313.1945.

The epidithioketopiperazines *anti*-**4a**, *syn*-**4b**, *anti*-**5a** and *syn*-**5b**, were synthesized according to the methodology reported by Nicolaou (Scheme S1).[S5, S6] The procedures described here were not optimized.

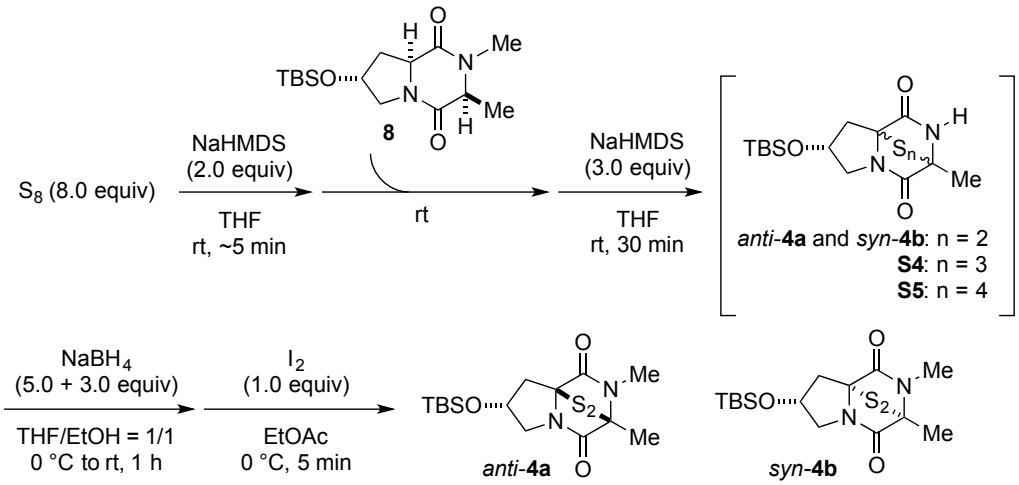

To a suspension of elemental sulfur S_8 (26.5 mg, 830 μmol) in THF (520 μL, 0.2 M) at room temperature under argon was added dropwise NaHMDS (310 μL, 1 M in THF) over a couple of minutes. The color changed from yellow to dark blue, dark orange and finally to light orange, and to the resulting solution was added dropwise a solution of **8** (32.4 mg, 104 μmol) in tetrahydrofuran (520 μL, 0.2 M) at room temperature over a couple of minutes, until the reaction mixture turned light brown. Then, additional NaHMDS (310 μL, 1 M in THF) was added and the resulting mixture was stirred for 30 min at room temperature. The reaction mixture was quenched with saturated $NHCl_4$aq (5 mL), and the aqueous layer was extracted with dichloromethane (10 mL × 3). The combined organic layer was dried over anhydrous sodium sulfate and concentrated *in vacuo*. The reaction mixture was roughly purified by flash column chromatography (hexane/ethyl acetate = 100/0 to 70/30) to give a mixture of products, including epidithiodiketopiperazine *anti*-**4a** and *syn*-**4b**, epitrithiodiketopiperazines **S4** and epitetrathiodiketopiperazines **S5** (24.3 mg). The crude mixture was dissolved in degassed tetrahydrofuran/ethanol (1/1, 1.11 mL, 50 mM) at 0 °C. To the stirred solution was added $NaBH_4$ (10.5 mg, 277 μmol) under argon and stirring was continued at room temperature. The reaction was monitored by reversed-phase TLC (hexane/ethyl acetate = 1/2), and after stirring for 1 h, the reaction was not completed. Therefore, further $NaBH_4$ (6.3 mg, 166 μmol) was added at room temperature and the reaction mixture was stirred for 5 min at room temperature. Upon completion of the reaction, the solution was cooled to 0 °C, quenched by addition of saturated aqueous ammonium chloride (2 mL), and extracted with ethyl acetate (5 mL × 3). The combined organic layer was dried over anhydrous sodium sulfate

and concentrated *in vacuo*. To a solution of the crude product in ethyl acetate (5 mL) was added 1.0 equivalent of I_2 in ethyl acetate (0.55 mL). The mixture was stirred for 5 min at 0 °C, then quenched with 10% aqueous sodium thiosulfate solution (3 mL), and the resulting mixture was extracted with ethyl acetate (5 mL × 3). The combined organic layer was dried over anhydrous sodium sulfate and concentrated *in vacuo*. The residue was purified by flash column chromatography (hexane/ethyl acetate = 100/0 to 90/10) to give *anti*-**4a** (9.2 mg, 3 steps 24%) together with *syn*-**4b** (5.0 mg, 3 steps 13%). The relative stereochemistry of *anti*-**4a** was determined by X-ray analysis (See, **Figure S1** and **Table S1**).

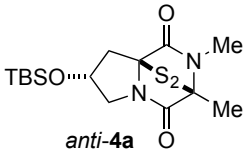

anti-**4a**

^{1}H NMR (400 MHz, $CDCl_3$) δ 4.77–4.72 (m, 1H), 3.93 (dd, J = 11.6, 5.9 Hz, 1H), 3.55 (dd, J = 11.7, 4.8 Hz), 3.09 (dd, J = 14.5, 6.2 Hz, 1H), 3.05 (s, 3H), 2.50 (dd, J = 14.7, 6.0 Hz), 1.98 (s, 3H), 0.87 (s, 9H), 0.11 (s, 3H), 0.09 (s, 3H); **^{13}C NMR** (100 MHz, $CDCl_3$) δ 165.9, 163.1, 73.8, 73.5, 69.6, 53.3, 41.8, 27.3, 25.6, 18.3, 17.9, –4.9, –5.0; **$[\alpha]_D^{27}$** +94 (*c* 0.9, $CHCl_3$); **FTIR** (neat) 2953, 2929, 2894, 2856, 1693 cm^{-1}; **HRMS-ESI** calcd for $C_{15}H_{27}N_2O_3SiS_2$: 375.1232, found: 375.1235.

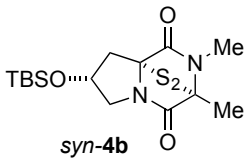

syn-**4b**

^{1}H NMR : (400 MHz, $CDCl_3$) δ 4.65–4.56 (m, 1H), 3.88 (dd, J = 11.7, 5.7 Hz, 1H), 3.68 (dd, J = 12.0, 3.2 Hz, 1H), 3.25 (dd, J = 14.7, 6.0 Hz, 1H), 3.04 (s, 3H), 2.31 (dd, J = 14.7, 3.7 Hz), 1.97 (s, 3H), 0.90 (s, 9H), 0.11 (s, 3H), 0.09 (s, 3H); **^{13}C NMR** (100 MHz, $CDCl_3$) δ 166.2, 163.2, 73.4, 73.0, 69.0, 53.9, 42.0, 27.3, 25.6, 18.3, 17.9, –4.8, –4.9; **$[\alpha]_D^{27}$** –122 (*c* 0.5, $CHCl_3$); **FTIR** (neat) 2953, 2930, 2857, 1694 cm^{-1}; **HRMS-ESI** calcd for $C_{15}H_{26}N_2O_3SiS_2Na$: 397.1052, found: 397.1047.

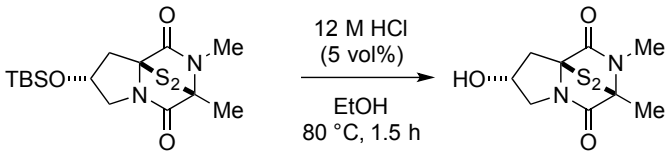

anti-**4a** *anti*-**5a**

To a solution of *anti*-**4a** (5.8 mg, 15.5 μmol) in EtOH (730 μL, 20 mM) was added 12 M HCl (40 μL) at room temperature. The mixture was heated to 80 ºC, and stirring for 1.5 h at 80 ºC. Then, the reaction was quenched with saturated sodium hydrogen carbonate (0.5 mL) at room temperature, and the whole was extracted with ethyl acetate (2 mL x 3). The combined organic layers were dried over anhydrous sodium sulfate. After evaporation of the solvent, the residue was purified by flash column chromatography (hexane/ethyl acetate = 2/1) to give *anti*-**5a** (3.6 mg, 90%).

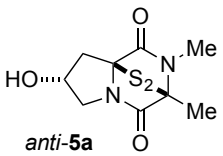

anti-**5a**

^{1}H NMR (400 MHz,

$CDCl_3$) δ 4.79–4.75 (m, 1H), 3.88 (dd, J = 12.2, 4.8 Hz, 1H), 3.79 (ddd, J = 12.4, 2.8, 1.4 Hz, 1H), 3.25 (dd, J = 14.9, 3.7, 0.9 Hz, 1H), 3.06 (s, 3H), 2.56 (dd, J = 14. 7, 5.5 Hz, 1H), 1.99 (s, 3H); **^{13}C NMR** (100 MHz, $CDCl_3$) δ 166.3, 163.4, 73.8, 73.6, 69.6, 53.1, 41.7, 27.4, 18.3; **$[\alpha]_D^{23}$** +105 (*c* 0.4, $CHCl_3$); FTIR (neat): 3433 (br), 2929, 1681 cm^{-1}; **HRMS-ESI** calcd for $C_9H_{12}N_2O_3S_2Na$: 283.0187, found: 283.0188.

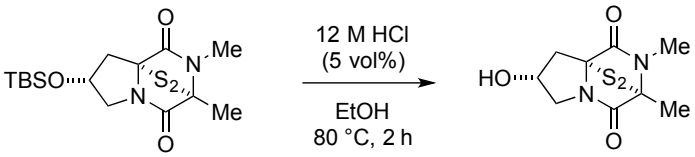

syn-**4b** *syn*-**5b**

To a solution of *syn*-**4b** (2.5 mg, 6.67 μmol) in EtOH (640 μL) was added 12 M HCl (30 μL) at room temperature. The mixture was heated to 80 ºC and stirred at the same temperature for 2.0 h. Then, the reaction was quenched with saturated sodium hydrogen carbonate (0.5 mL) at room temperature, and the mixture was extracted with ethyl acetate (2 mL x 3). The combined organic layer was dried over anhydrous sodium sulfate. After evaporation of the solvent, the residue was purified by flash column chromatography (hexane/ethyl acetate = 1/2) to give *syn*-**5b** (1.5 mg, 88%). In order to obtain sufficient solubility of *syn*-**5b**, THF-d_8 was used for ^{13}C NMR.

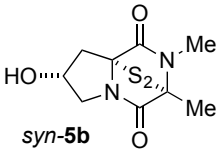

syn-**5b**

^{1}H NMR (400 MHz, $CDCl_3$) δ 4.68 (tt, J = 5.1, 1.4 Hz, 1H), 3.94 (dt, J = 12.6, 1.8 Hz), 3.86 (dd, 12.9, 5.1 Hz, 1H), 3.23 (dd, J = 15.6, 5.5 Hz, 1H), 3.06 (s, 3H), 2.49 (dt, J = 15.6, 1.38 Hz, 1H), 2.00 (s, 3H); **^{13}C NMR** (100 MHz, THF-d_8) δ165.8, 162.6, 74.1, 73.6, 68.1, 53.6, 41.7, 26.1, 17.6; **$[\alpha]_D^{24}$** –153 (*c* 0.2, EtOH); **FTIR** (neat) 3431 (br), 2923, 1680 cm^{-1}; **HRMS-ESI** calcd for $C_9H_{12}N_2O_3S_2Na$: 283.0187, found: 283.0189.

3. X-Ray analysis of *anti*-4a

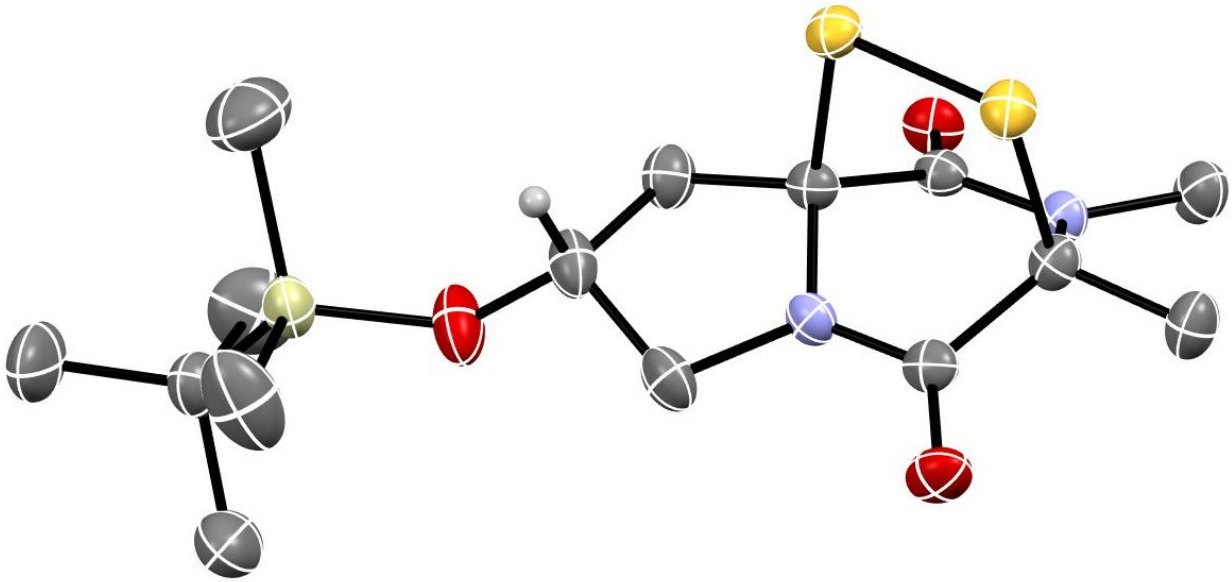

Figure S1. **ORTEP drawing of *anti*-4a (CCDC 1825180).** H atoms are omitted for the sake of clarity, except on the chiral carbon.

Table S1. Crystal data and structure refinement for *anti*-4a

Empirical formula	$C_{15}H_{26}N_2O_3S_2Si$
Formula weight	374.59
Temperature	170 K
Wavelength	1.54187 Å
Crystal system	Orthorhombic
Space group	$P2_12_12_1$
Unit cell dimensions	a = 7.68141(14) Å
	b = 10.8441(2) Å
	c = 23.4756(4) Å
V	1955.48(6) Å^3
Z	4
D_X	1.272 Mg/m^3
Absorption coefficient	3.177 mm^{-1}
F(000)	800
Crystal size	0.83 x 0.16 x 0.14 mm^3
Theta range for data collection	3.77 to 68.24°.
Index ranges	$-9 \le h \le 8$, $-13 \le k \le 13$, $-28 \le l \le 28$
Reflections collected	21681
Independent reflections	3550 [R_{int} = 0.0421]
Completeness to theta = 68.24°	99.5 %
Absorption correction	Numerical
Max. and min. transmission	0.6879 and 0.2858
Refinement method	Full-matrix least-squares on F^2
Data / restraints / parameters	3550 / 0 / 217
Goodness-of-fit on F^2	1.081
Final R indices [$I>2\sigma(I)$]	$R(F)$ = 0.0267, $wR(F^2)$ = 0.0656
R indices (all data)	$R(F)$ = 0.0278, $wR(F^2)$ = 0.0661
Absolute structure parameter	–0.012(5)
Largest diff. peak and hole	0.216 and -0.189 e.Å^{-3}

4. Synthesis of ProSeAM (1)

ProSeAM (**1**)[S7-S8] was synthesized as reported [S9] with a few modifications, especially for purification (**Scheme S2**). In our procedure, Sep-Pak® (Waters Sep-Pak® Vac 6cc C18-500mg cartridge) and/or reversed-phase HPLC were used to obtain reproducibility in the synthesis of (*S*)-selenohomocystine (**S6**) and (*S*)-Se-adenosylselenohomocysteine (SeAH: **S7**). The reaction conditions described here were not optimized.

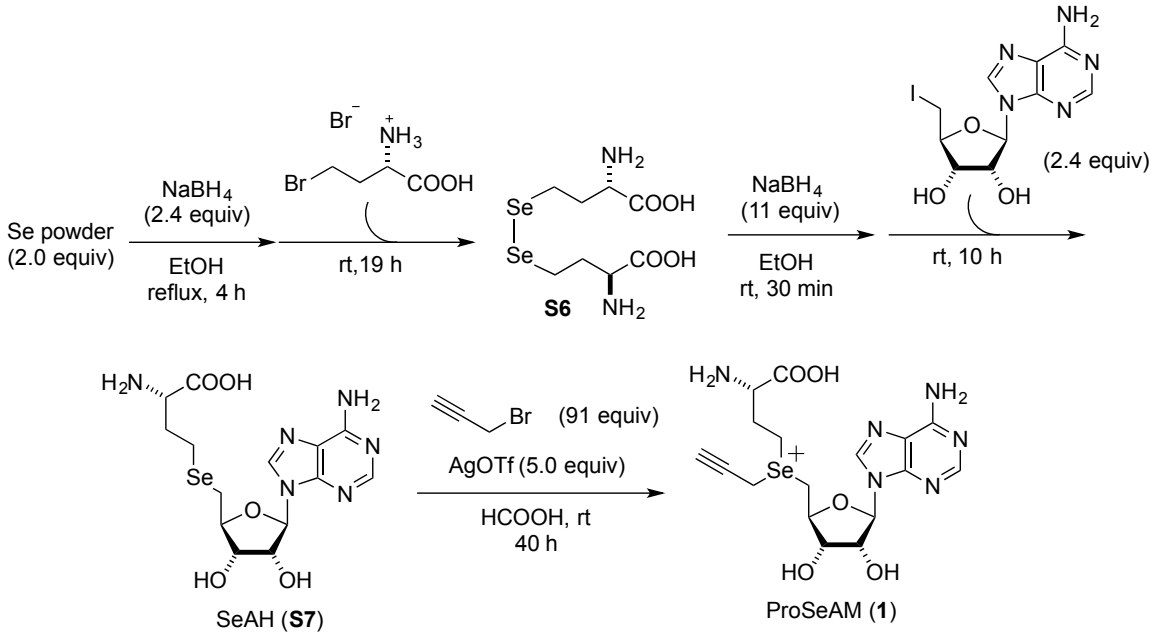

Scheme S2. Synthetic scheme for ProSeAM (1).

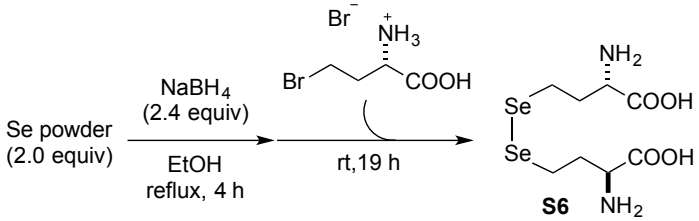

Se powder (135.7 mg, 1.72 mmol) was suspended in EtOH (15 mL) at room temperature. The suspension was stirred at 95 °C under reflux in an Ar atmosphere (balloon) for 15 min. To the resulting suspension was added $NaBH_4$ (77.4 mg, 2.04 mmol) at 95 °C, and stirring was continued for 4 h at 95 °C under Ar. The reaction mixture was cooled to room temperature, and (*S*)-2-amino-4-bromobutyric acid hydrobromide (225.9 g, 0.86 mmol), purchased from Aldrich, was added to it. After further stirring for 19 h at room temperature under Ar, the reaction was quenched with 2 M HCl (2.0 mL). The solid precipitate was collected on a paper filter, and washed with H_2O containing 0.1% TFA. The filtrate was concentrated by rotary evaporation. The residue was dissolved in H_2O containing 0.1%TFA, and then purified by reversed-phase HPLC using a Senshu

Pak PEGASIL ODS100 (ϕ10 x 250 mm) with 16% MeOHaq containing 0.1% TFA (3.0 mL/min flow rate, detected at 254 nm, 20 °C, t_r 11.9 min). The fraction containing **S6** was concentrated in a freeze-dryer to give **S6** in 89% yield (138.2 mg, 0.38 mmol). The NMR spectrum of **S6** was consistent with reported data.[S9]

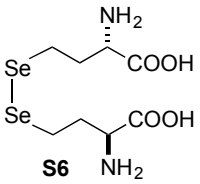

S6

^{1}NMR [400 MHz, D_2O containing 0.1% TFA (pH ~2)] δ 4.14 (t, J = 6.4 Hz, 2H), 3.06–2.96 (m, 4H), 2.49–2.31 (m, 4H); **^{13}C NMR** [100 MHz, D_2O containing 0.1% TFA (pH ~2)] δ 172.0, 52.9, 31.4, 22.7.

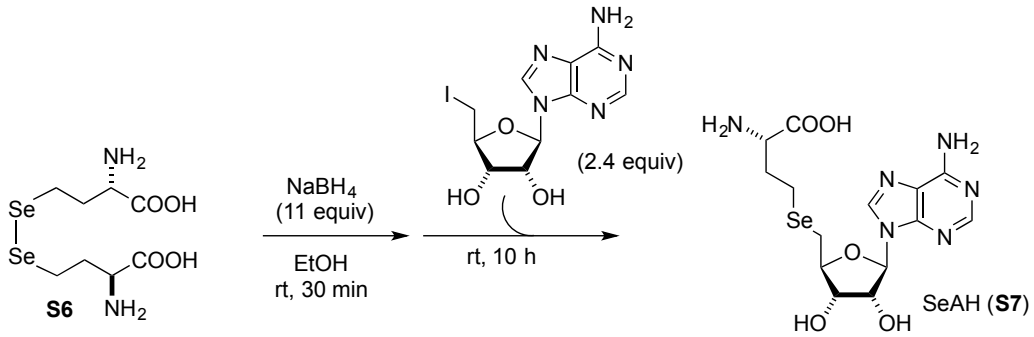

To a solution of **S6** (36.6 mg, 0.101 mol) in EtOH was added $NaBH_4$ (43.0 mg, 1.13 mnol) at room temperature under Ar. The mixture was stirred for 30 min at room temperature, than 5'-iodo-5'-deoxyadenosine[S9] (91.5 mg, 0.243 mmol) was added at room temperature under Ar, and stirring was continued for 10 h. The solvent was removed in a rotary evaporator, and the residue was dissolved in H_2O and roughly purified using Sep-Pak® (Waters Sep-Pak® Vac 6cc C18-500mg cartridge) with stepwise elution (H_2O, 2.5% MeOHaq, 10% MeOHaq, 50% MeOHaq and 100% MeOH). Fractions (2.5% MeOHaq, and 10% MeOHaq) containing SeAH (**S7**) were combined and freeze-dried to give SeAH (**S7**) in 18% yield (15.6 mg, 0.036 mmol). The ^{1}H and ^{13}C NMR spectra of **S7** were consistent with reported data. [S9]

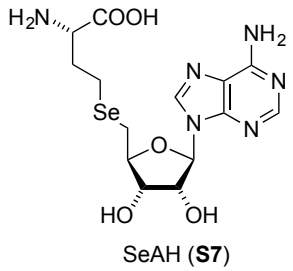

SeAH (**S7**)

^{1}H NMR [400 MHz, D_2O containing 0.1% TFA (pH ~2)] δ 8.53 (s, 1H), 8.44 (s, 1H), 6.14 (d, J = 4.6 Hz, 1H), 4.88 (dd, J = 9.9, 4.8 Hz, 1H), 4.42 (t, J = 5.1 Hz, 1H), 4.39–4.35 (m, 1H), 4.09 (t, J = 6.2 Hz, 1H), 3.09 (dd, J = 13.3, 5.1 Hz, 1H), 3.03 (dd, J = 13.3, 6.9 Hz, 1H), 2.72 (t, J = 7.81 Hz, 2H), 2.34–2.15 (m, 2H). **^{13}C NMR** [100 MHz, D_2O containing 0.1% TFA (pH ~2)] δ 172.5, 150.1, 148.4, 144.7, 142.9, 119.0, 88.4, 84.2, 73.7, 73.0, 53.4, 31.0, 25.4, 18.8; **HRMS-ESI** $[M+H]^+$ calcd for $C_{14}H_{21}N_6O_5Se$: 433.0733, found 433.0734, $[M+Na]^+$ calcd for $C_{14}H_{21}N_6O_5NaSe$: 455.0553, found 433.0542.

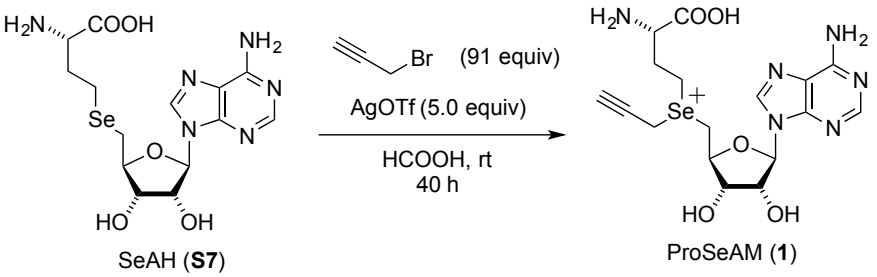

SeAH (**S7**) ProSeAM (**1**)

SeAH (**S7**: 15.6 mg, 36 μmol) was dissolved in formic acid (720 μL), and the mixture was stirred at 0 ˚C for 15 min. To the mixture were added propargyl bromide (164 μL, 2.18 mmol, 61 equiv) and silver triflate (29.3 mg, 0.114 mmol) at 0 ˚C. The mixture was allowed to warm to room temperature, and stirred for 22 h in a reaction flask protected from sunlight. Monitoring by reversed-phase TLC (10% MeOH) showed that SeAH (**S7**) still remained. Therefore, additional propargyl bromide (82 μL, 1.09 mmol) and silver triflate (16.9 mg, 0.066 mmol) dissolved in formic acid (100 μL), were added and stirring was continued for a further 18 h. Upon complete consumption of SeAH (**S7**), the reaction mixture was diluted with water (4 mL), and then washed with diethyl ether (5 mL x 3). Freeze-drying afforded a residue, which was dissolved in H_2O and roughly purified by Sep-Pak® (Waters Sep-Pak® Vac 6cc C18-500mg cartridge) with stepwise elution (H_2O, 50% MeOHaq, and 100% MeOH) in order to remove excess silver triflate. The eluate was freeze-dried. Because isolated ProSeAM (**1**) is unstable under neutral or basic conditions,[S7, S8] **1** was dissolved in H_2O or D_2O, and which pH was controlled at about 2 with TFA, as follows. The residue was dissolved in H_2O (pH controlled to about 2 with TFA), and then purified by reversed-phase HPLC using an ATLANTIS™ T3C18 (ϕ10 x 250 mm) column with 5% MeOHaq containing 0.1% TFA (2.0 ml/min flow rate, detected at 254 nm, 20 °C) to selectively give two diastereomers of the corresponding propargylated adduct, at 15.0 min (high polar adduct) and 15.9 min (less polar adduct). We used the biologically active fraction (less polar adduct at 15.9 min) in this study; this fraction was concentrated by freeze-drying to give ProSeAM (**1**) in 3.5 % yield (0.6 mg, 1.3 μmol; calculated on the basis of the formula $C_{17}H_{23}N_6O_5Se$ without considering the counter anion). To avoid decomposition of isolated ProSeAM (**1**), the sample dissolved in D_2O (the pH was controlled to about 2 with TFA) and directly transferred from the NMR tube to an Eppendorf tube without removing D_2O (the pH was controlled about 2 with TFA, 2.1 mM). The stock solution (2.1 mM) in D_2O (the pH was controlled about 2 with TFA) was kept in a deep freezer. All the biological assays described below were conducted using samples diluted with 2 mM TFA in H_2O.

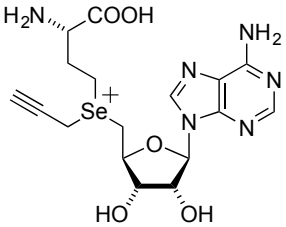

ProSeAM (**1**)

^{1}H NMR [400 MHz, D_2O containing 0.1% TFA (pH ~2)] δ 8.47 (s, 1 H), 8.47 (s, 1H) 6.16 (d, J = 3.7 Hz), 4.67–4.53 (m, 1 H), 4.21 (br d, J = 1.4 Hz, 2H), 4.00 (dd, J = 12.6, 3.4 Hz, 1H), 3.96–3.90 (m, 2H), 3.67–3.52 (m, 2H), 3.22 (t, J = 2.6 Hz, 1H), 2.46–2.35 (m, 2H), 2.21 (s, 2H); **HRMS-ESI** calcd for $C_{17}H_{23}N_6O_5Se$: 471.0896, found 471.0898.

5. Assay for PMT-inhibitory activity of ETPs using ProSeAM (1): Fig 3b

HEK293T cell lysate (30 μg) in 3 μL of lysis buffer (50 mM Tris-HCl, pH 8.0, 50 mM KCl, 10% glycerol, 0.1% Tween-20) was mixed with 0.5 μL of the indicated concentrations of ETPs in **1** x reaction buffer (50 mM Tris-HCl, pH 8.0, total reaction volume was 19.5 μL), and incubated for 10 min at rt. Then, 0.5 μL of 2 mM ProSeAM (final concentration was 50 μM) was added to the reaction tube and incubation was continued for 2 h at 20 °C; in all cases, ProSeAM (**1**) was freshly prepared. The reaction was stopped by adding four volumes of ice-cold acetone. The reaction tube was centrifuged at 15,000 x g for 5 min, and the precipitate was washed once with ice-cold acetone. The pellet was resolved in 15.5 μL of 1 x PBS +0.2% SDS, then 4 μL of 5 x click reaction buffer and 0.5 μL of 10 mM Azide-PEG4-Biotin (Click Chemistry Tools: Bioconjugate Technology Company, Scottsdale, AZ, USA) were added, and the mixture was incubated for 60 min at rt. The click reaction was stopped with four volumes of ice-cold acetone. The pellet was resolved in 10 μL of Laemmli SDS-sample buffer. Proteins were separated on 12.5% acrylamide gel and transferred to a nitrocellulose membrane (Pall Corporation, Port Washington, NY, USA), which was then incubated with streptavidin-HRP (Thermo Fisher Scientific Inc., Waltham, MA, USA) for 1 h at rt. The membrane was washed three times with 1× PBS, and incubated with the Western Lightning Plus-ECL Kit (Perkin Elmer, Waltham MA, USA) according to the manufacturer's protocol. Chemiluminescence was detected with X-ray film (RX-U, Fuji Film, Minato-ku, Tokyo, Japan). Signal intensity of bands was measured with ImageJ software. IC_{50} values for histone were calculated from the intensity of the 17 kDa band, and those for non-histones from the integrated band intensity from 20 kDa to 250 kDa. The signal intensity of anti-α-tubulin was used for normalization as a loading control. Three experiments were conducted independently, and IC_{50} values are shown as mean ± SEM.

Table S2. IC_{50} values of ETPs **4**, **5** and chaetocin (**2**).

	IC_{50} [μM] (Histone)	IC_{50} [μM] (Non-histone)
anti-**4a**	2.63 ± 0.41	31.6 ± 21.3
syn-**4b**	55.3 ± 16	78.1 ± 14.5
anti-**5a**	6.68 ± 1.4	10.3 ± 3.61
syn-**5b**	34.8 ± 10.3	6.25 ± 1.11
2	2.21 ± 0.79	6.02 ± 2.38

6. Quantitative MS/MS analysis for identification of protein substrates: Fig 4a

HEK293T cells were cultured for at least six doubling times in DMEM+10% dialyzed FBS containing either light-carbon-containing lysine (12C) or stable-isotope-labeled (13C) lysine with a SILAC labeling kit (Pierce # 89983). The lysates (150 μg) in lysis buffer (50 mM Tris-HCl, pH 8.0, 50 mM KCl, 10% glycerol, 0.1% Tween-20) were mixed with (13C) or without (12C) 250 μM labeled *syn*-**5b** in 1 x reaction buffer (50 mM Tris- HCl, pH 8.0), and incubated for 10 min at rt. Then 250 μM ProSeAM (**1**) was added to the reaction tube and incubation was continued for 2 h at 20 °C. The reaction was stopped by adding four volumes of ice-cold acetone. The reaction tube was centrifuged at 15,000 x g for 5 min, and the precipitate was washed once with ice-cold acetone. The pellet was resolved in 39 μL of 1× PBS + 0.2% SDS, then 10 μL of 5× click reaction buffer and 1 μL of 10 mM Azide-PEG4-Biotin (Click Chemistry Tools) were added. The mixture was incubated for 60 min at rt. The click reaction was stopped with four volumes of ice-cold acetone. The pellet was resolved in 75 μL of binding buffer (1× PBS, 0.1% Tween-20, 2% SDS, 20 mM DTT) and sonicated for 10 s. The 12C and 13C samples were mixed in one tube, then 3 mg of Dynabeads M-280 Streptavidin (Life Technologies Japan Ltd., Minato-ku, Tokyo, Japan) in 450 μL of IP buffer (TBS, 0.1% Tween-20) was added, and the mixture was incubated for 30 min at rt (the final SDS concentration in the reaction mixture was 0.5%). The protein-bound beads were washed 3 times with wash buffer (1× PBS, 0.1% Tween-20, 0.5% SDS) and then washed twice more with 100 mM ammonium bicarbonate (ABC) buffer. The protein-bound beads were analyzed by mass spectrometry. Acetonitrile (1/10 volume) and DTT (20 mM) were added to the protein-bound Dynabeads in 100 mM ABC buffer, and the mixture was incubated for 30 min at 56 °C. Then, iodoacetamide (IAA) was added and the mixture was incubated for 30 min at 37 °C in the dark. The protein samples were digested with 1 μg Lys-C (Promega), and the protein fragments were applied to a liquid chromatograph (EASY-nLC 1000; Thermo Fisher Scientific, Odense, Denmark) coupled to a Q Exactive Hybrid Quadrupole-Orbitrap Mass Spectrometer (Thermo Fisher Scientific, Inc., San Jose, CA, USA) with a nanospray ion source in the positive mode. The peptides were separated on a NANO-HPLC capillary column C18 (0.075-mm inner diameter 150 mm length, 3 mm particle size; Nikkyo Technos, Tokyo, Japan). Mobile phase ‘‘A’’ was comprised of water with 0.1% formic acid, and mobile phase ‘‘B’’ was comprised of acetonitrile with 0.1% formic acid. Two different slopes were used for a 120 min gradient at a flow rate of 300 nL/ min: 0%–30% B in 100 min and then 30%–65% B in 100-120 min. The parameters of the mass spectrometer were as follows: spray voltage, 2.3 kV; capillary temperature, 275 °C; mass-to-charge ratio, 350–1800; normalized collision energy, 28%. Raw data were acquired with the Xcalibur software (Thermo Fisher Scientific). The MS and MS/MS data were searched against the Swiss-Prot database using Proteome Discoverer 1.4 (Thermo Fisher Scientific) with the MASCOT search engine

software, version 2.4.1 (Matrix Science, London, United Kingdom). The search parameters were as follows: enzyme, Lys-C; quantitation, SILAC K (+6); static modifications, carbamidomethyl (Cys); dynamic modifications, oxidation (Met); precursor mass tolerance, 6 ppm; fragment mass tolerance, 20 mDa; maximum missed cleavages, 1. The proteins were considered identified when the false discovery rates (FDR) were less than 1%. For substrate identification, proteins with at least a 2-fold decrease were defined as hit protein targets against *syn*-**5b**. In total, 90 proteins were identified as substrates of *syn*-**5b** sensitive MTases (**Table S3**).

Table S3. List of protein substrates, whose intensities are decreased at least 2-fold by *syn*-**5b**

Accession	Description	Score	Coverage	Heavy/ Light	Heavy/Light Count	Heavy/Light Variability [%]	MW [kDa]
Q71U36	Tubulin alpha-1A chain OS=Homo sapiens GN=TUBA1A PE=1 SV=1 - [TBA1A_HUMAN]	694.1	29.7	0.113	10	10.6	50.1
P07437	Tubulin beta chain OS=Homo sapiens GN=TUBB PE=1 SV=2 - [TBB5_HUMAN]	545.3	32.7	0.148	15	27.1	49.6
Q12906	Interleukin enhancer-binding factor 3 OS=Homo sapiens GN=ILF3 PE=1 SV=3 - [ILF3_HUMAN]	521.3	15.4	0.440	12	10.8	95.3
Q05519	Serine/arginine-rich splicing factor 11 OS=Homo sapiens GN=SRSF11 PE=1 SV=1 - [SRS11_HUMAN]	387.6	17.4	0.398	8	23.7	53.5
P13667	Protein disulfide-isomerase A4 OS=Homo sapiens GN=PDIA4 PE=1 SV=2 - [PDIA4_HUMAN]	360.3	30.9	0.169	14	46.4	72.9
P13645	Keratin, type I cytoskeletal 10 OS=Homo sapiens GN=KRT10 PE=1 SV=6 - [K1C10_HUMAN]	323.6	20.7	0.019	3	101.2	58.8
O43175	D-3-phosphoglycerate dehydrogenase OS=Homo sapiens GN=PHGDH PE=1 SV=4 - [SERA_HUMAN]	308.7	22.3	0.456	11	19.5	56.6
P61978	Heterogeneous nuclear ribonucleoprotein K OS=Homo sapiens GN=HNRNPK PE=1 SV=1 - [HNRPK_HUMAN]	306.1	17.1	0.343	6	11.4	50.9
Q92945	Far upstream element-binding protein 2 OS=Homo sapiens GN=KHSRP PE=1 SV=4 - [FUBP2_HUMAN]	297.9	14.8	0.252	8	14.1	73.1
P08670	Vimentin OS=Homo sapiens GN=VIM PE=1 SV=4 - [VIME_HUMAN]	293.9	14.4	0.487	8	9.3	53.6
P12268	Inosine-5'-monophosphate dehydrogenase 2 OS=Homo sapiens GN=IMPDH2 PE=1 SV=2 - [IMDH2_HUMAN]	287.8	15.0	0.469	8	17.4	55.8
P36578	60S ribosomal protein L4 OS=Homo sapiens GN=RPL4 PE=1 SV=5 - [RL4_HUMAN]	222.4	18.5	0.344	7	17.2	47.7
P53396	ATP-citrate synthase OS=Homo sapiens GN=ACLY PE=1 SV=3 - [ACLY_HUMAN]	210.7	13.9	0.410	11	9.8	120.8
O00410	Importin-5 OS=Homo sapiens GN=IPO5 PE=1 SV=4 - [IPO5_HUMAN]	206.8	7.2	0.485	6	38.8	123.5
Q00839	Heterogeneous nuclear ribonucleoprotein U OS=Homo sapiens GN=HNRNPU PE=1 SV=6 - [HNRPU_HUMAN]	204.7	13.1	0.369	8	30.1	90.5
Q16881	Thioredoxin reductase 1, cytoplasmic OS=Homo sapiens GN=TXNRD1 PE=1 SV=3 - [TRXR1_HUMAN]	199.1	19.3	0.021	5	68.5	70.9
P45880	Voltage-dependent anion-selective channel protein 2 OS=Homo sapiens GN=VDAC2 PE=1 SV=2 - [VDAC2_HUMAN]	195.0	17.7	0.267	3	9.6	31.5
P10599	Thioredoxin OS=Homo sapiens GN=TXN PE=1 SV=3 - [THIO_HUMAN]	186.4	23.8	0.427	3	11.0	11.7
Q8NEC7	Glutathione S-transferase C-terminal domain-containing protein OS=Homo sapiens GN=GSTCD PE=1 SV=2 - [GSTCD_HUMAN]	177.6	4.4	0.312	6	3.6	71.0
Q99986	Serine/threonine-protein kinase VRK1 OS=Homo sapiens GN=VRK1 PE=1 SV=1 - [VRK1_HUMAN]	177.5	14.7	0.427	5	15.8	45.4
P30101	Protein disulfide-isomerase A3 OS=Homo sapiens GN=PDIA3 PE=1 SV=4 - [PDIA3_HUMAN]	177.2	28.1	0.248	9	41.4	56.7
Q08J23	tRNA (cytosine(34)-C(5))-methyltransferase OS=Homo sapiens GN=NSUN2 PE=1 SV=2 - [NSUN2_HUMAN]	168.1	14.1	0.445	7	47.7	86.4
O60613	15 kDa selenoprotein OS=Homo sapiens GN=SEP15 PE=1 SV=3 - [SEP15_HUMAN]	161.9	24.1	0.015	1		17.8
O95232	Luc7-like protein 3 OS=Homo sapiens GN=LUC7L3 PE=1 SV=2 - [LC7L3_HUMAN]	159.0	19.0	0.373	5	5.1	51.4
P41252	Isoleucine--tRNA ligase, cytoplasmic OS=Homo sapiens GN=IARS PE=1 SV=2 - [SYIC_HUMAN]	155.5	6.3	0.303	5	16.3	144.4
P07237	Protein disulfide-isomerase OS=Homo sapiens GN=P4HB PE=1 SV=3 - [PDIA1_HUMAN]	137.1	10.2	0.194	6	50.4	57.1
P27635	60S ribosomal protein L10 OS=Homo sapiens GN=RPL10 PE=1 SV=4 - [RL10_HUMAN]	136.6	21.0	0.118	3	28.2	24.6
P27816	Microtubule-associated protein 4 OS=Homo sapiens GN=MAP4 PE=1 SV=3 - [MAP4_HUMAN]	130.7	8.1	0.236	5	3.2	120.9
P49411	Elongation factor Tu, mitochondrial OS=Homo sapiens GN=TUFM PE=1 SV=2 - [EFTU_HUMAN]	128.9	17.7	0.485	6	24.2	49.5
P18583	Protein SON OS=Homo sapiens GN=SON PE=1 SV=4 - [SON_HUMAN]	112.9	3.0	0.366	5	94.2	263.7
O75369	Filamin-B OS=Homo sapiens GN=FLNB PE=1 SV=2 - [FLNB_HUMAN]	112.0	2.2	0.374	3	13.3	278.0
O15355	Protein phosphatase 1G OS=Homo sapiens GN=PPM1G PE=1 SV=1 - [PPM1G_HUMAN]	110.2	4.0	0.422	2	26.6	59.2
Q15084	Protein disulfide-isomerase A6 OS=Homo sapiens GN=PDIA6 PE=1 SV=1 - [PDIA6_HUMAN]	105.6	7.1	0.180	2	3.4	48.1
P22102	Trifunctional purine biosynthetic protein adenosine-3 OS=Homo sapiens GN=GART PE=1 SV=1 - [PUR2_HUMAN]	105.0	10.9	0.497	5	11.8	107.7
P08243	Asparagine synthetase [glutamine-hydrolyzing] OS=Homo sapiens GN=ASNS PE=1 SV=4 - [ASNS_HUMAN]	103.2	11.2	0.281	4	19.6	64.3
P14866	Heterogeneous nuclear ribonucleoprotein L OS=Homo sapiens GN=HNRNPL PE=1 SV=2 - [HNRPL_HUMAN]	103.1	17.2	0.496	6	22.0	64.1
P41250	Glycine--tRNA ligase OS=Homo sapiens GN=GARS PE=1 SV=3 - [SYG_HUMAN]	102.2	6.1	0.226	5	18.1	83.1
P0CG48	Polyubiquitin-C OS=Homo sapiens GN=UBC PE=1 SV=3 - [UBC_HUMAN]	95.2	31.5	0.263	3	26.4	77.0
P31943	Heterogeneous nuclear ribonucleoprotein H OS=Homo sapiens GN=HNRNPH1 PE=1 SV=4 - [HNRH1_HUMAN]	91.6	16.3	0.388	6	14.5	49.2
P58546	Myotrophin OS=Homo sapiens GN=MTPN PE=1 SV=2 - [MTPN_HUMAN]	90.6	17.0	0.329	2	11.9	12.9
P26599	Polypyrimidine tract-binding protein 1 OS=Homo sapiens GN=PTBP1 PE=1 SV=1 - [PTBP1_HUMAN]	89.8	12.8	0.221	3	14.0	57.2
P30837	Aldehyde dehydrogenase X, mitochondrial OS=Homo sapiens GN=ALDH1B1 PE=1 SV=3 - [AL1B1_HUMAN]	89.4	5.2	0.364	3	8.2	57.2
P18621	60S ribosomal protein L17 OS=Homo sapiens GN=RPL17 PE=1 SV=3 - [RL17_HUMAN]	89.4	22.3	0.098	4	27.1	21.4
Q8NBS9	Thioredoxin domain-containing protein 5 OS=Homo sapiens GN=TXNDC5 PE=1 SV=2 - [TXND5_HUMAN]	86.4	10.7	0.178	2	51.6	47.6
Q9H7Z7	Prostaglandin E synthase 2 OS=Homo sapiens GN=PTGES2 PE=1 SV=1 - [PGES2_HUMAN]	79.8	9.6	0.239	3	23.6	41.9
P83731	60S ribosomal protein L24 OS=Homo sapiens GN=RPL24 PE=1 SV=1 - [RL24_HUMAN]	77.6	15.3	0.059	2	3.2	17.8
O75582	Ribosomal protein S6 kinase alpha-5 OS=Homo sapiens GN=RPS6KA5 PE=1 SV=1 - [KS6A5_HUMAN]	76.4	4.7	0.157	3	5.9	89.8
Q13523	Serine/threonine-protein kinase PRP4 homolog OS=Homo sapiens GN=PRPF4B PE=1 SV=3 - [PRP4B_HUMAN]	75.8	3.5	0.404	3	11.4	116.9
Q96AG4	Leucine-rich repeat-containing protein 59 OS=Homo sapiens GN=LRRC59 PE=1 SV=1 - [LRC59_HUMAN]	75.6	8.8	0.474	2	18.9	34.9
Q9HA64	Ketosamine-3-kinase OS=Homo sapiens GN=FN3KRP PE=1 SV=2 - [KT3K_HUMAN]	73.4	14.2	0.349	4	39.1	34.4
Q15181	Inorganic pyrophosphatase OS=Homo sapiens GN=PPA1 PE=1 SV=2 - [IPYR_HUMAN]	73.2	13.8	0.178	2	7.6	32.6
Q9Y383	Putative RNA-binding protein Luc7-like 2 OS=Homo sapiens GN=LUC7L2 PE=1 SV=2 - [LC7L2_HUMAN]	72.2	6.6	0.340	2	32.7	46.5
P15170	Eukaryotic peptide chain release factor GTP-binding subunit ERF3A OS=Homo sapiens GN=GSPT1 PE=1 SV=1 - [ERF3A_HUMAN]	70.3	7.2	0.221	2	15.0	55.7
Q9HBK9	Arsenite methyltransferase OS=Homo sapiens GN=AS3MT PE=1 SV=3 - [AS3MT_HUMAN]	70.2	20.3	0.022	1		41.7
Q9BVP2	Guanine nucleotide-binding protein-like 3 OS=Homo sapiens GN=GNL3 PE=1 SV=2 - [GNL3_HUMAN]	70.1	6.9	0.178	3	10.3	62.0
Q8WUM4	Programmed cell death 6-interacting protein OS=Homo sapiens GN=PDCD6IP PE=1 SV=1 - [PDC6I_HUMAN]	70.1	6.7	0.391	4	17.7	96.0
P39023	60S ribosomal protein L3 OS=Homo sapiens GN=RPL3 PE=1 SV=2 - [RL3_HUMAN]	68.4	8.7	0.163	3	48.4	46.1
P53618	Coatomer subunit beta OS=Homo sapiens GN=COPB1 PE=1 SV=3 - [COPB_HUMAN]	65.5	4.2	0.297	2	46.0	107.1
P42166	Lamina-associated polypeptide 2, isoform alpha OS=Homo sapiens GN=TMPO PE=1 SV=2 - [LAP2A_HUMAN]	65.2	8.1	0.025	3	167.8	75.4
P55265	Double-stranded RNA-specific adenosine deaminase OS=Homo sapiens GN=ADAR PE=1 SV=4 - [DSRAD_HUMAN]	64.7	3.8	0.330	3	49.4	136.0
P54136	Arginine--tRNA ligase, cytoplasmic OS=Homo sapiens GN=RARS PE=1 SV=2 - [SYRC_HUMAN]	64.2	8.6	0.489	4	38.9	75.3
Q15717	ELAV-like protein 1 OS=Homo sapiens GN=ELAVL1 PE=1 SV=2 - [ELAV1_HUMAN]	64.0	7.4	0.459	1		36.1
Q13310	Polyadenylate-binding protein 4 OS=Homo sapiens GN=PABPC4 PE=1 SV=1 - [PABP4_HUMAN]	63.0	7.5	0.480	3	47.1	70.7
P84098	60S ribosomal protein L19 OS=Homo sapiens GN=RPL19 PE=1 SV=1 - [RL19_HUMAN]	62.2	22.5	0.243	4	14.3	23.5
P49792	E3 SUMO-protein ligase RanBP2 OS=Homo sapiens GN=RANBP2 PE=1 SV=2 - [RBP2_HUMAN]	61.0	2.0	0.132	2	31.6	358.0
Q16891	MICOS complex subunit MIC60 OS=Homo sapiens GN=IMMT PE=1 SV=1 - [MIC60_HUMAN]	60.7	3.3	0.495	2	19.9	83.6
P29966	Myristoylated alanine-rich C-kinase substrate OS=Homo sapiens GN=MARCKS PE=1 SV=4 - [MARCS_HUMAN]	60.0	10.8	0.279	2	9.2	31.5
Q15021	Condensin complex subunit 1 OS=Homo sapiens GN=NCAPD2 PE=1 SV=3 - [CND1_HUMAN]	57.7	2.0	0.244	2	42.8	157.1
P23526	Adenosylhomocysteinase OS=Homo sapiens GN=AHCY PE=1 SV=4 - [SAHH_HUMAN]	57.6	5.6	0.362	2	48.6	47.7
P46087	Probable 28S rRNA (cytosine(4447)-C(5))-methyltransferase OS=Homo sapiens GN=NOP2 PE=1 SV=2 - [NOP2_HUMAN]	55.8	4.3	0.433	3	5.4	89.2
Q13263	Transcription intermediary factor 1-beta OS=Homo sapiens GN=TRIM28 PE=1 SV=5 - [TIF1B_HUMAN]	55.6	11.4	0.315	6	20.0	88.5
Q9BQG0	Myb-binding protein 1A OS=Homo sapiens GN=MYBBP1A PE=1 SV=2 - [MBB1A_HUMAN]	53.9	1.7	0.354	2	29.2	148.8
P78527	DNA-dependent protein kinase catalytic subunit OS=Homo sapiens GN=PRKDC PE=1 SV=3 - [PRKDC_HUMAN]	52.9	1.9	0.479	5	12.8	468.8
Q9Y678	Coatomer subunit gamma-1 OS=Homo sapiens GN=COPG1 PE=1 SV=1 - [COPG1_HUMAN]	51.9	6.5	0.483	4	4.9	97.7
P46060	Ran GTPase-activating protein 1 OS=Homo sapiens GN=RANGAP1 PE=1 SV=1 - [RAGP1_HUMAN]	49.9	8.0	0.496	2	2.2	63.5
Q14204	Cytoplasmic dynein 1 heavy chain 1 OS=Homo sapiens GN=DYNC1H1 PE=1 SV=5 - [DYHC1_HUMAN]	47.4	0.8	0.300	2	10.0	532.1
Q6UWP8	Suprabasin OS=Homo sapiens GN=SBSN PE=1 SV=2 - [SBSN_HUMAN]	43.7	4.8	0.041	2	119.9	60.5
Q8NI27	THO complex subunit 2 OS=Homo sapiens GN=THOC2 PE=1 SV=2 - [THOC2_HUMAN]	43.5	1.5	0.333	2	9.8	182.7
P38432	Coilin OS=Homo sapiens GN=COIL PE=1 SV=1 - [COIL_HUMAN]	43.1	3.1	0.056	2	63.0	62.6
P06753	Tropomyosin alpha-3 chain OS=Homo sapiens GN=TPM3 PE=1 SV=2 - [TPM3_HUMAN]	42.8	8.4	0.120	1		32.9
P61247	40S ribosomal protein S3a OS=Homo sapiens GN=RPS3A PE=1 SV=2 - [RS3A_HUMAN]	40.0	11.4	0.480	1		29.9
Q15233	Non-POU domain-containing octamer-binding protein OS=Homo sapiens GN=NONO PE=1 SV=4 - [NONO_HUMAN]	39.4	5.1	0.468	3	17.0	54.2
P30048	Thioredoxin-dependent peroxide reductase, mitochondrial OS=Homo sapiens GN=PRDX3 PE=1 SV=3 - [PRDX3_HUMAN]	39.0	20.3	0.500	2	39.3	27.7
P17844	Probable ATP-dependent RNA helicase DDX5 OS=Homo sapiens GN=DDX5 PE=1 SV=1 - [DDX5_HUMAN]	38.7	3.6	0.442	2	6.5	69.1
O00571	ATP-dependent RNA helicase DDX3X OS=Homo sapiens GN=DDX3X PE=1 SV=3 - [DDX3X_HUMAN]	36.5	4.1	0.400	2	19.9	73.2
Q9Y2L1	Exosome complex exonuclease RRP44 OS=Homo sapiens GN=DIS3 PE=1 SV=2 - [RRP44_HUMAN]	35.6	3.9	0.455	2	4.5	108.9
O15042	U2 snRNP-associated SURP motif-containing protein OS=Homo sapiens GN=U2SURP PE=1 SV=2 - [SR140_HUMAN]	33.3	3.2	0.019	1		118.2
P49189	4-trimethylaminobutyraldehyde dehydrogenase OS=Homo sapiens GN=ALDH9A1 PE=1 SV=3 - [AL9A1_HUMAN]	29.9	8.1	0.272	1		53.8
P21108	Ribose-phosphate pyrophosphokinase 3 OS=Homo sapiens GN=PRPS1L1 PE=1 SV=2 - [PRPS3_HUMAN]	27.4	7.6	0.456	2	11.1	34.8
P27708	CAD protein OS=Homo sapiens GN=CAD PE=1 SV=3 - [PYR1_HUMAN]	22.3	1.9	0.074	2	669.2	242.8

7. Purification of recombinant PRMT1 and HNRNPK

Full-length cDNA corresponding to mouse PRMT1 (NCBI ID: NM_019830) and mouse HNRNPK (NCBI ID: NM_001301341) were obtained by PCR from a C57BL/6 mouse cDNA library. The cDNAs obtained were cloned into the pET19b vector to generate N-terminal His-tagged constructs (pET19b-PRMT1, pET19b-HNRNPK). *Escherichia coli* BL21 (pLysS) strains were transformed with pET19b plasmids, and the bacteria were cultured in 2× YT medium with ampicillin (100 μg/mL) and 0.2 mM isopropyl β-D-1-thiogalactopyranoside (IPTG) for 18-24 h at 16 °C. The cells were pelleted and lysed with 1× PBS/0.5% NP-40 by sonication with a Branson Sonifier (S-250D, Branson Ultrasonics Corp., CT, USA) for 5 min on ice. The lysates were centrifuged at 15,000 × g for 10 min, and the supernatants were incubated with Ni-NTA Agarose (Qiagen, Valencia, CA, USA) for 1 h at 4 °C with gentle agitation. The agarose beads were washed 5 times with wash buffer (50 mM Tris-HCl, pH 7.4, 25 mM imidazole) and then eluted with elution buffer (50 mM Tris-HCl pH 7.4, 250 mM imidazole). The purified proteins were dialyzed with 1× PBS/10% glycerol, and their concentration was measured using the Bradford Protein Assay Kit (BioRad Laboratories, Hercules, CA, USA).

8. Effect of *anti*-4a and *syn*-5b on PRMT-1-catalyzed methylation of HNRNPK: Fig 4b

HNRNPK (1 μg) was incubated in 1× Reaction buffer (50 mM Tris-HCl pH 8.0, reaction volume was 20 μL) with His-PRMT1 (0.2 μg) and the indicated amounts of inhibitors for 20 min at rt. SAM (20 μM final) was then added to the reaction tube and incubation was continued for 20 min at 30 °C. The reaction was stopped by adding Laemmli SDS-sample buffer. Proteins were resolved on a 10% acrylamide SDS-PAGE gel, and transferred to a nitrocellulose membrane (Pall Corporation, Port Washington, NY, USA). The membrane was incubated with anti-His antibody or anti-ADMA antibody overnight at 4 °C, then washed three times with 1xPBS/0.1% Tween20, incubated with appropriate HRP-conjugated secondary antibody for 1 h at rt, washed again three times with 1× PBS/0.1% Tween20, and incubated with the Western Lightning Plus-ECL Kit (Perkin Elmer, Waltham MA, USA) according to the manufacturer's protocol. Chemiluminescence was detected with X-ray film (RX-U, Fuji Film, Minato-ku, Tokyo, Japan). Antibodies used were obtained as follows: anti-6xHis antibody (Wako); anti-ADMA antibody (#13522, Cell Signaling Technology). IC_{50} values were calculated from the signal intensity of anti-ADMA antibody normalized to that of anti-His antibody. Four experiments were conducted independently IC_{50} values are shown as mean ± SEM.

9. Effect of *syn*-5b on HeLa cells:

HeLa cells ($2x10^5$) were seeded on 12-well plates, and cultured in DMEM with 10% FCS overnight at 37 °C, 5% CO_2. Cells were washed once with 1xPBS, then fresh DMEM with 10% FCS and *syn*-**5b** were added to each well. Cells were cultured for an additional 24 h and collected. Cell pellets were lysed with 20 µL Laemmli SDS-sample buffer. Proteins were resolved on a 12.5% acrylamide SDS-PAGE gel, and transferred to a nitrocellulose membrane for western blot analysis as described in section 8. Anti-α-tubulin antibody (clone B-5-1-2, Sigma-Aldrich, St. Louis, MO, USA) was used as a loading control for normalization of the intensity of anti-ADMA antibody. Three experiments were conducted independently. The determined IC_{50} value (22.7 ± 3.6 µM) is the mean ± SEM.

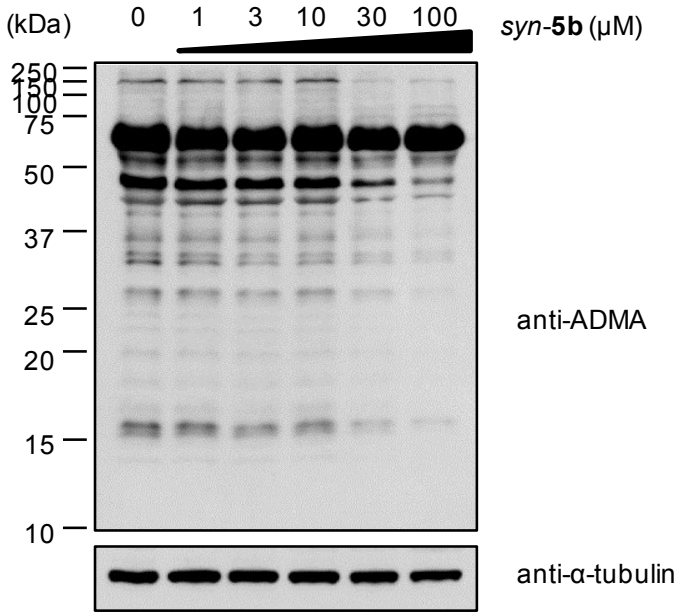

Figure S2. HeLa cells were treated with *syn*-**5b** at the indicated concentrations for 24 h

10. G9a-inhibitory activity of *anti*-4a, *syn*-4b, *anti*-5a and *syn*-5b

Inhibitory activities of compounds towards G9a was measured using an AlphaLISA enzymatic assay.[S10,S11] Briefly, recombinant human G9a proteins (final concentration 0.0675 nM) (BPS Bioscience, San Diego, CA, USA) were pre-treated with each compound for 10 min and then incubated with biotinylated histone H3 peptide (1-21) (final concentration 100 nM) and SAM (final concentration 15 μM) in 10 μL of assay buffer (50 mM Tris-HCl [pH 9.0], 50 mM NaCl, 0.01% Tween-20, 1 mM DTT). After 60 min at room temperature, anti-H3K9me2 acceptor beads (final concentration 20 μg/mL) and streptavidin donor beads (final concentration 20 μg/mL) were added and incubation was continued for 60 min at room temperature. The α signal was detected using an EnSpire Alpha plate reader (PerkinElmer, Waltham, MA, USA).

Table S4. G9a-inhibitory activity of ETPs *in vitro*

Entry	ETPs	IC_{50} [μM]
1	Chaetocin (**2**)	7.2 ± 0.37
2	*anti*-**4a**	1.2 ± 0.17
3	*syn*-**4b**	2.7 ± 0.65
4	*anti*-**5a**	1.4 ± 0.14
5	*syn*-**5b**	2.5 ± 0.60

We found significantly different inhibition trends of *syn*-**5b** between AlphaLISA enzymatic assay using G9a, which catalyzes H3K9 dimethlyation (Table S4), and chemical methylome assay using ProSeAM (**1**), shown in Figure 3 (main text). For example, in the AlphaLISA enzymatic assay, all of the newly developed chiral ETPs, *anti*-**4a**, *syn*-**4a**, *anti*-**5a** and *syn*-**5b**, showed slightly stronger G9a-inhibitory activity than the parent chaetocin (**2**). In marked contrast, when we assessed the ProSeAM (**1**)-mediated protein-labeling pattern upon treatment with ETPs as shown in Figure 3a (main text), *syn*-**5b** more strongly inhibited non-histone substrates than the histone bands, whereas other ETPs (*anti*-**4a**, *syn*-**4b** and *anti*-**5a**) inhibited histone bands rather than non-histone bands. Subsequent quantitative MS/MS analysis using **1** led to identification of the target substrate of *syn*-**5b** shown in Figure 4a (main text). Table S3 shows that the substrates of protein arginine methyltransferase (PRMT) constitute the majority, while those of PKMT are minor (methylation on only R: 17 proteins, both R and K: 4 proteins, only K: 3 proteins).

We would like to emphasize that the observed difference of inhibition trends of *syn*-**5b** between chemical methylome assay using ProSeAM (**1**) and AlphaLISA enzymatic assay using recombinant G9a highlights the advantage of chemical methylome analysis for identifying the targets of inhibitor candidates among poorly characterized PMT substrates. Further investigations to elucidate the molecular mechanism of the target selectivity switching between *syn*-**5b** and other ETPs are in progress.

11. Cytotoxicity of *anti*-4a, *syn*-4b, *anti*-5a and *syn*-5b

As we previously reported,[S1] the newly developed ETPs show far weaker cytotoxicity than chaetocin (**2**). COS-7 cells (2 x 10^3 cells/well) were seeded on 96-well plates, and cultured in DMEM with 10% FCS overnight at 37 °C, 5% CO_2. Cells were treated with test compounds for 72 h, then 10 μL of alamarBlue (Biosource International) was added to each well. The cell viability was determined based on the increase of fluorescence (excitation 560 nm/emission 590 nm) during 2-3 h incubation. IC_{50} values were calculated by Origin software, and data are presented as mean ± S.D. (n = 3, three independent experiments).

Table S5. Cytotoxicity of ETPs. COS-7 cells were treated with the ETPs over the course of 72 h, and cell viability was determined by alamarBlue assay.

Entry	ETPs	IC_{50} [μM]
1	Chaetocin (**2**)	0.26 ± 0.026
2	*anti*-**4a**	>30
3	*syn*-**4b**	>30
4	*anti*-**5a**	>30
5	*syn*-**5b**	>30

12. Copies of NMR Spectra

Compound 7

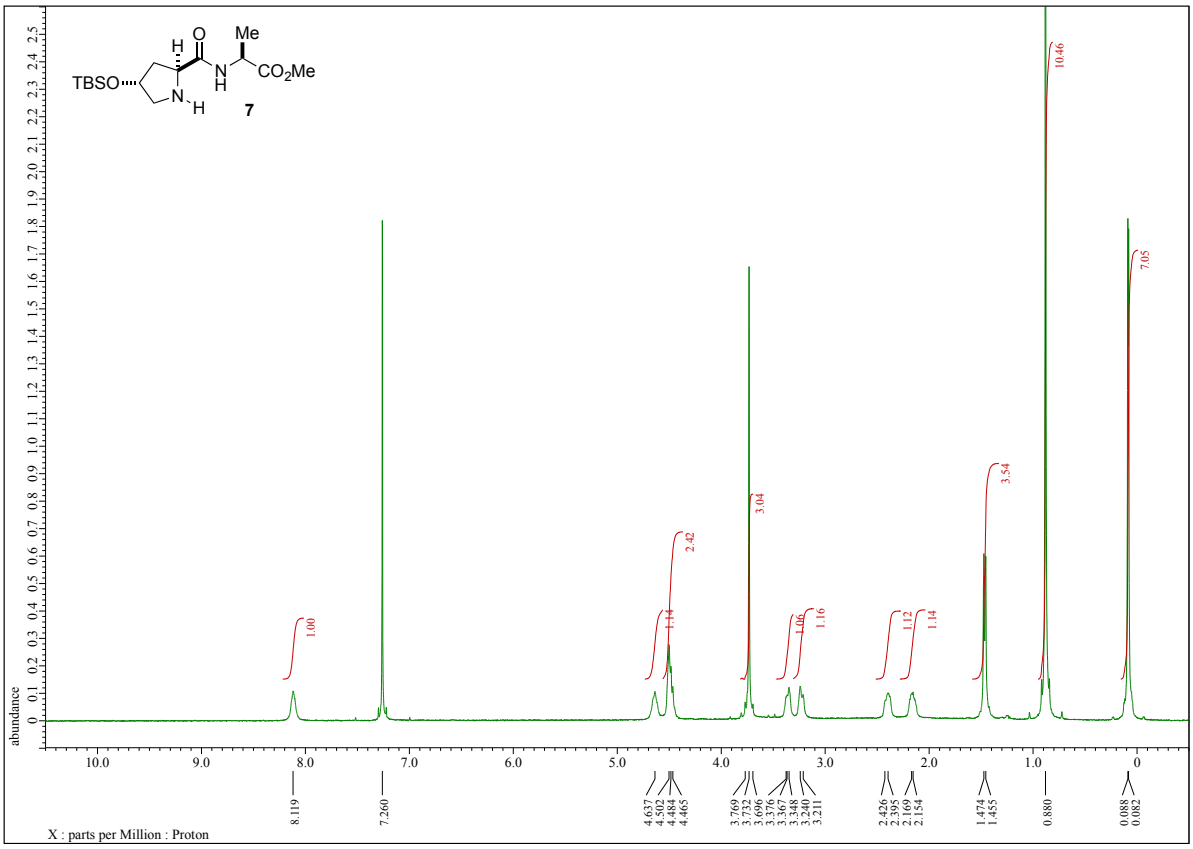

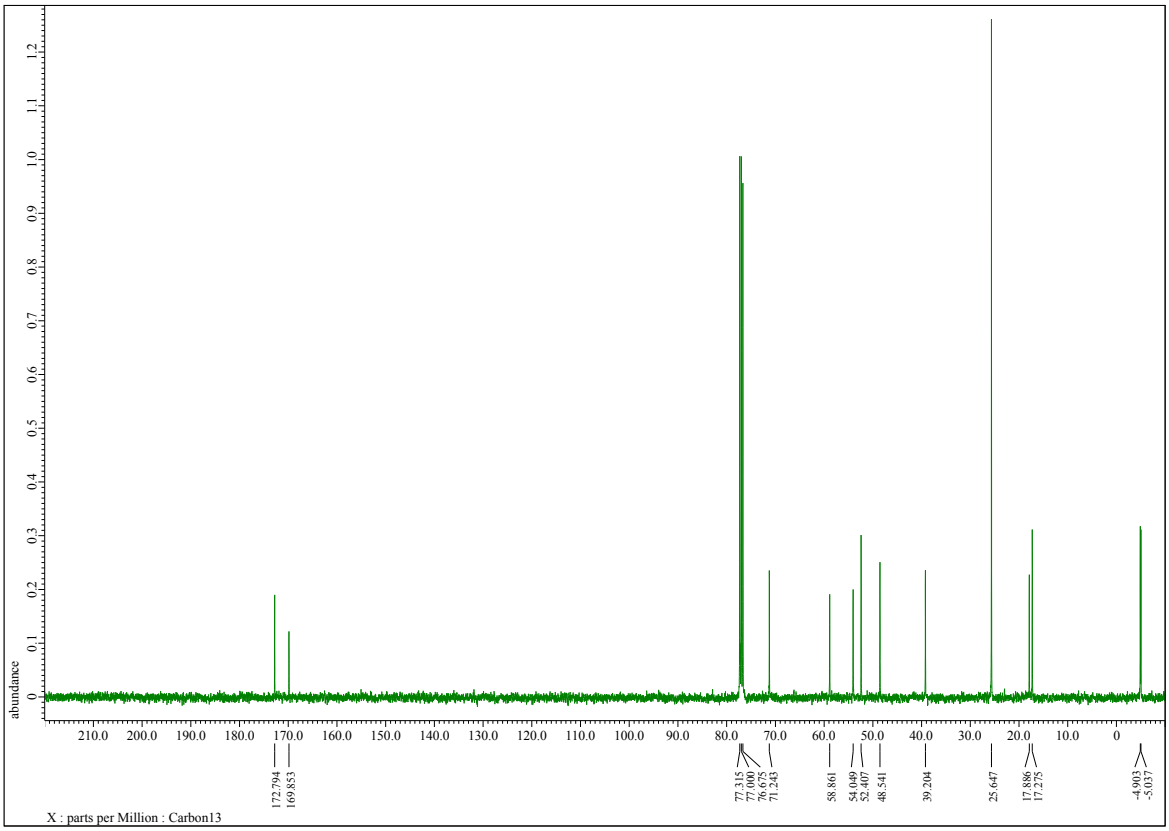

Compound 8

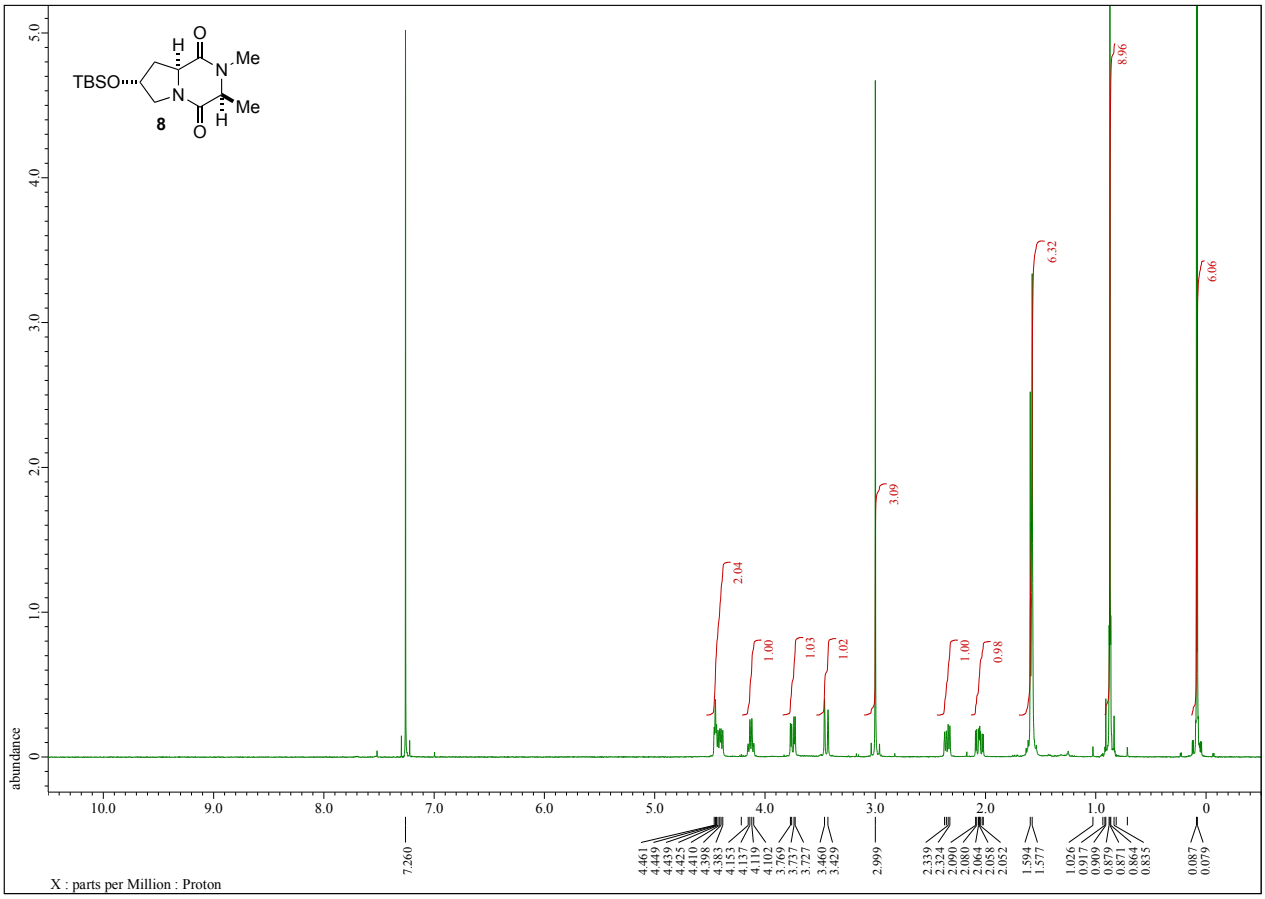
TBSO
Me
Me
8
abundance
X : parts per Million : Proton

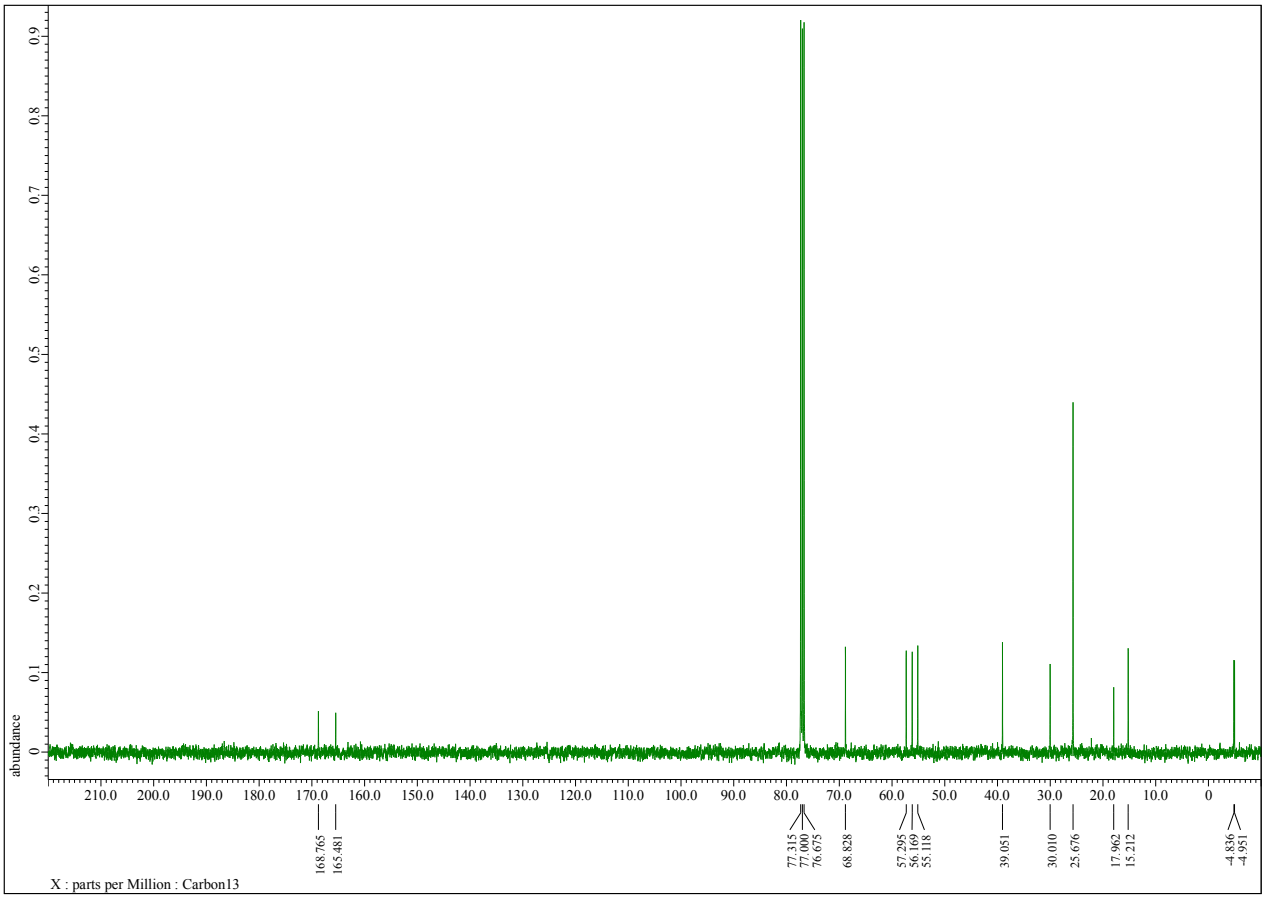
abundance
X : parts per Million : Carbon13

***anti*-4a**

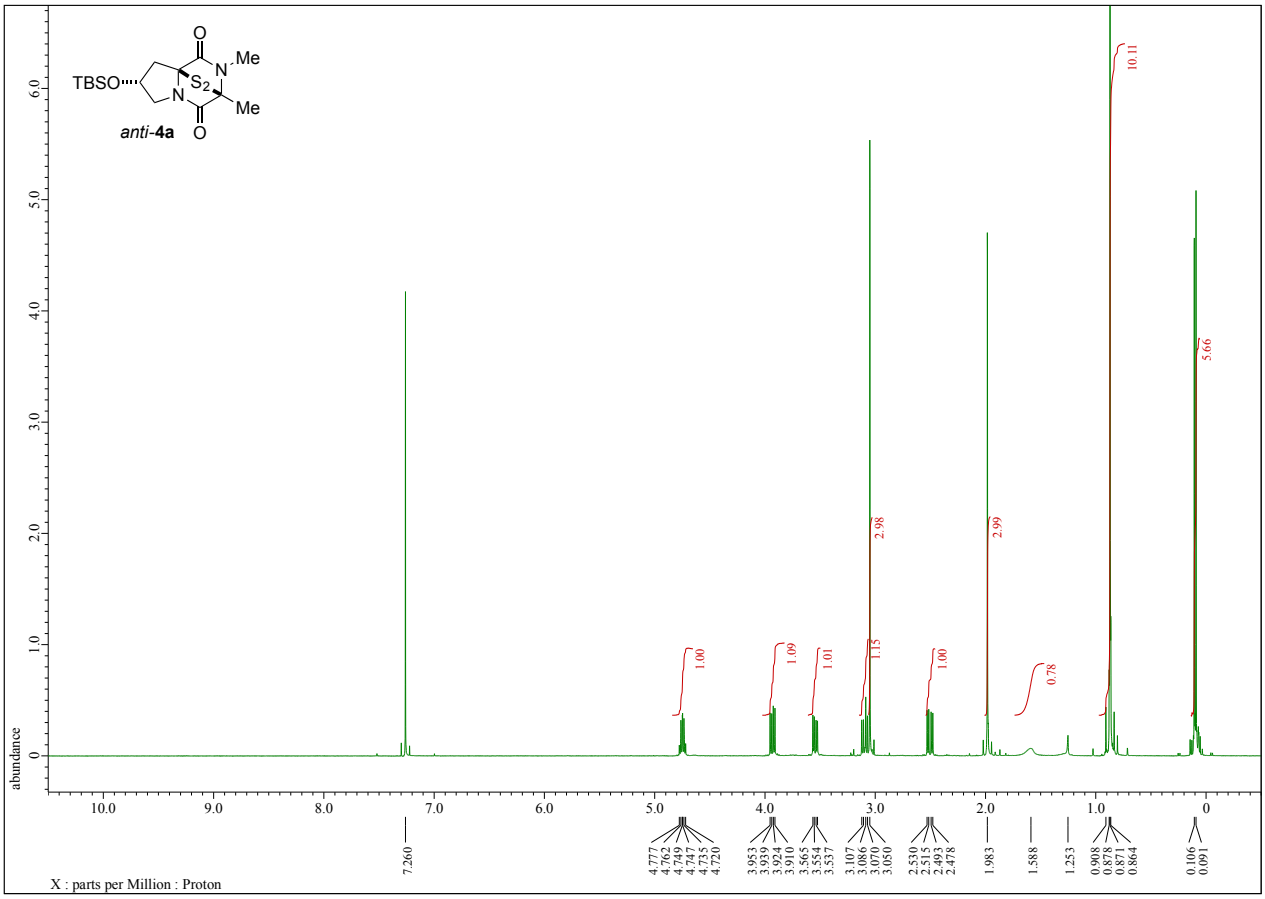
TBSO
Me
Me
anti-4a
abundance
X : parts per Million : Proton

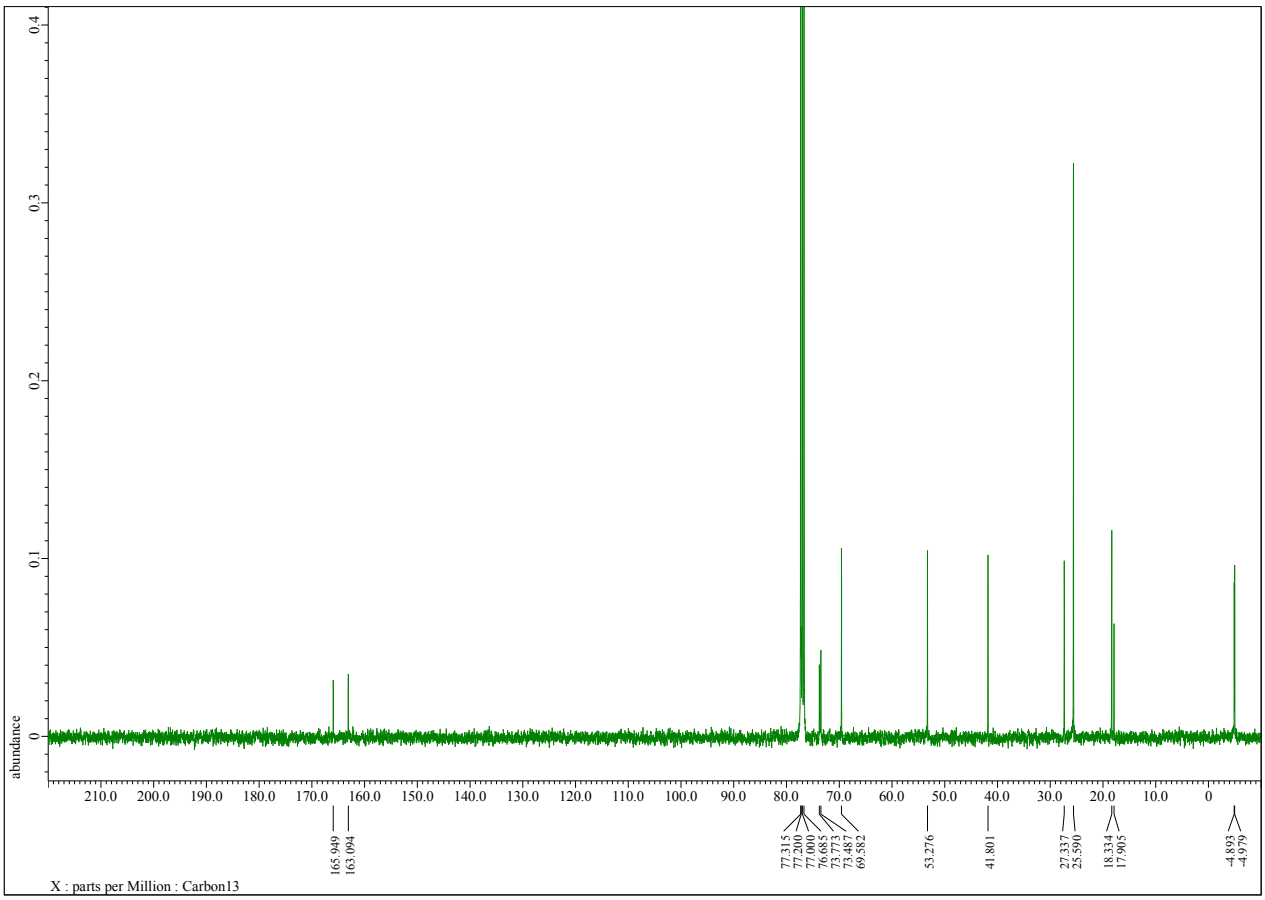
abundance
X : parts per Million : Carbon13

***syn*-4b**

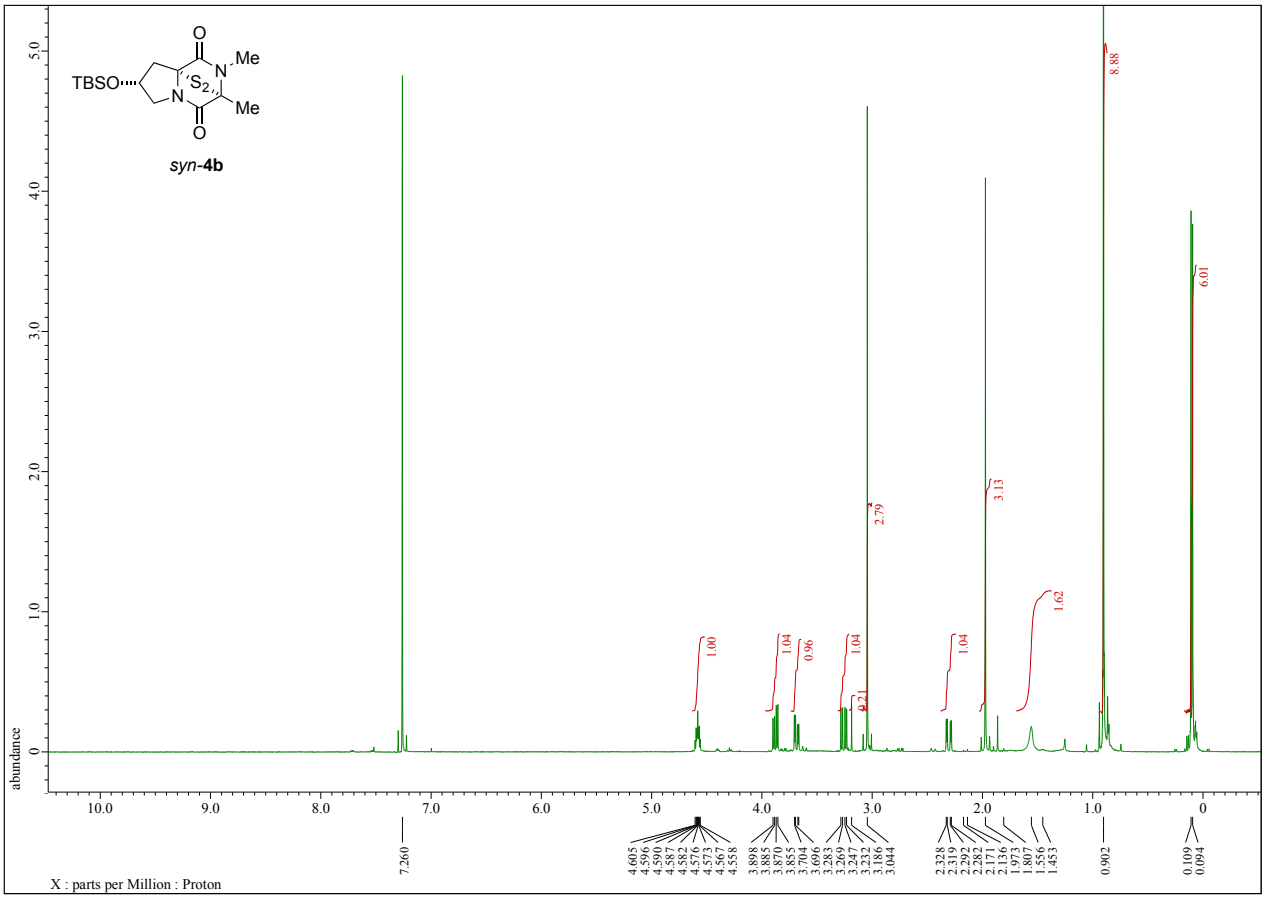
TBSO
Me
Me
syn-4b
abundance
X : parts per Million : Proton
1.00
1.04
0.96
1.04
2.79
1.04
3.13
1.62
8.88
6.01

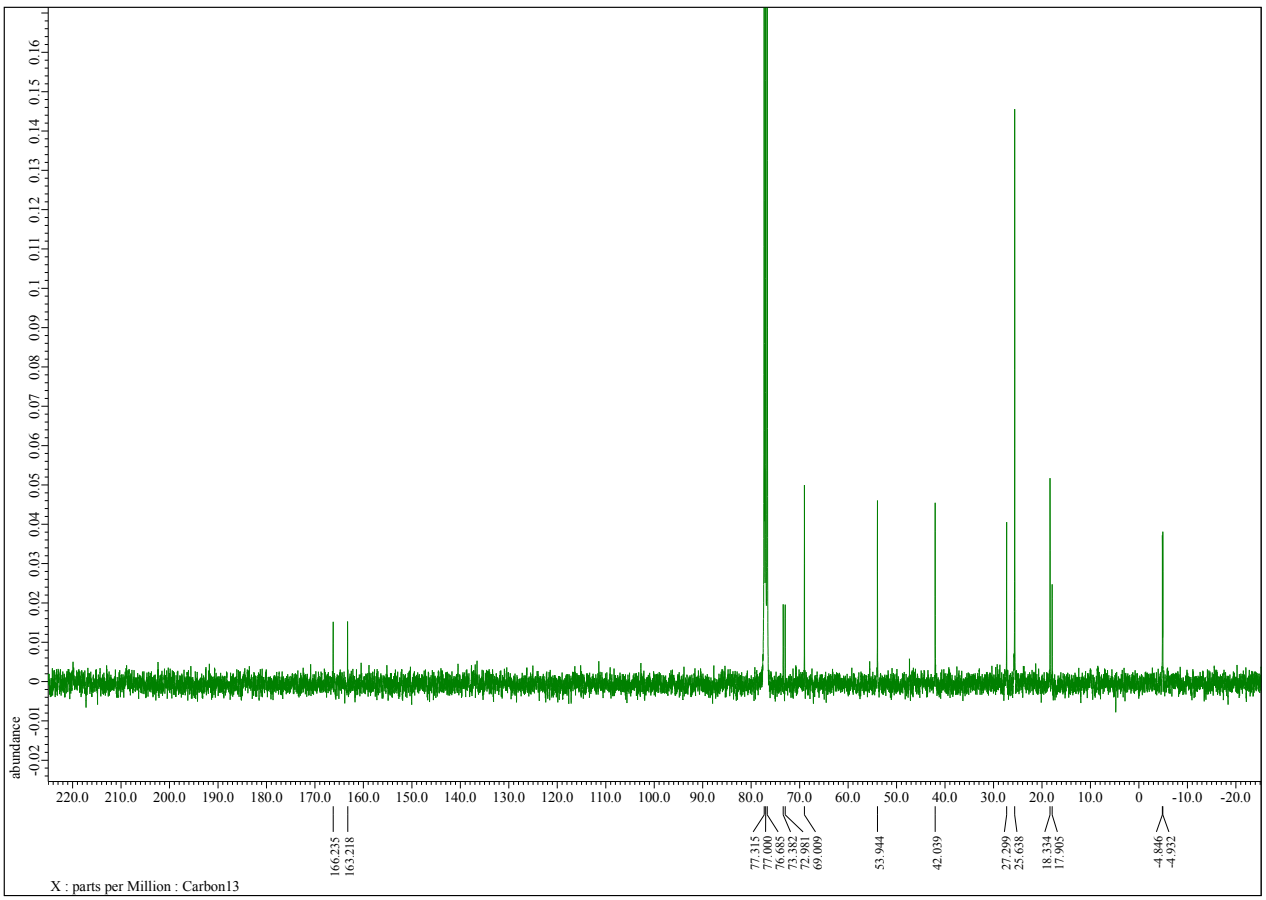
abundance
X : parts per Million : Carbon13

***anti*-5a**

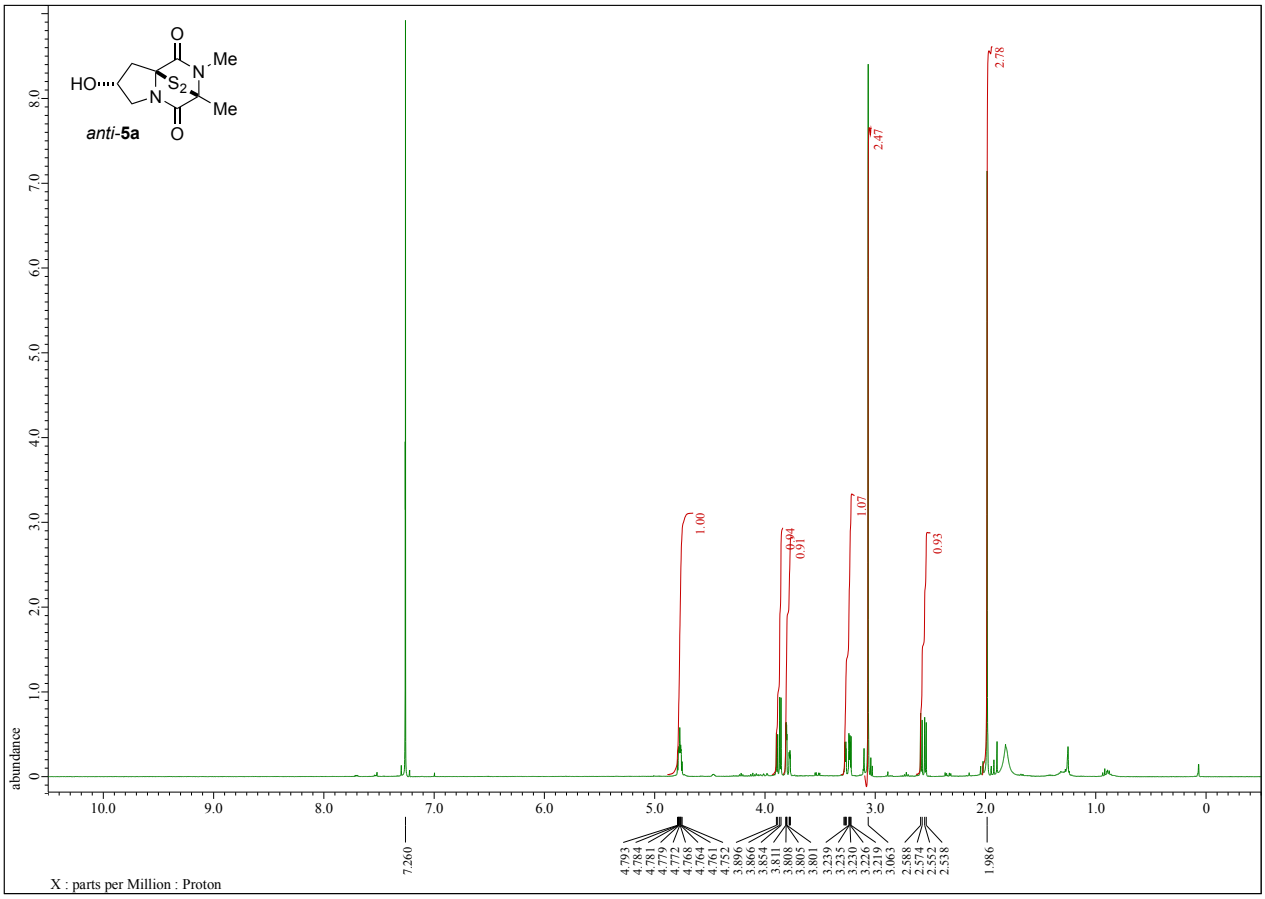
HO
O
N
Me
S2
N
Me
O
anti-5a
abundance
X : parts per Million : Proton
7.260
4.793
4.784
4.781
4.779
4.772
4.768
4.764
4.761
4.752
3.866
3.854
3.811
3.808
3.805
3.801
3.239
3.235
3.230
3.226
3.219
3.063
2.588
2.574
2.552
2.538
1.986
1.00
0.94
0.91
1.07
2.47
0.93
2.78

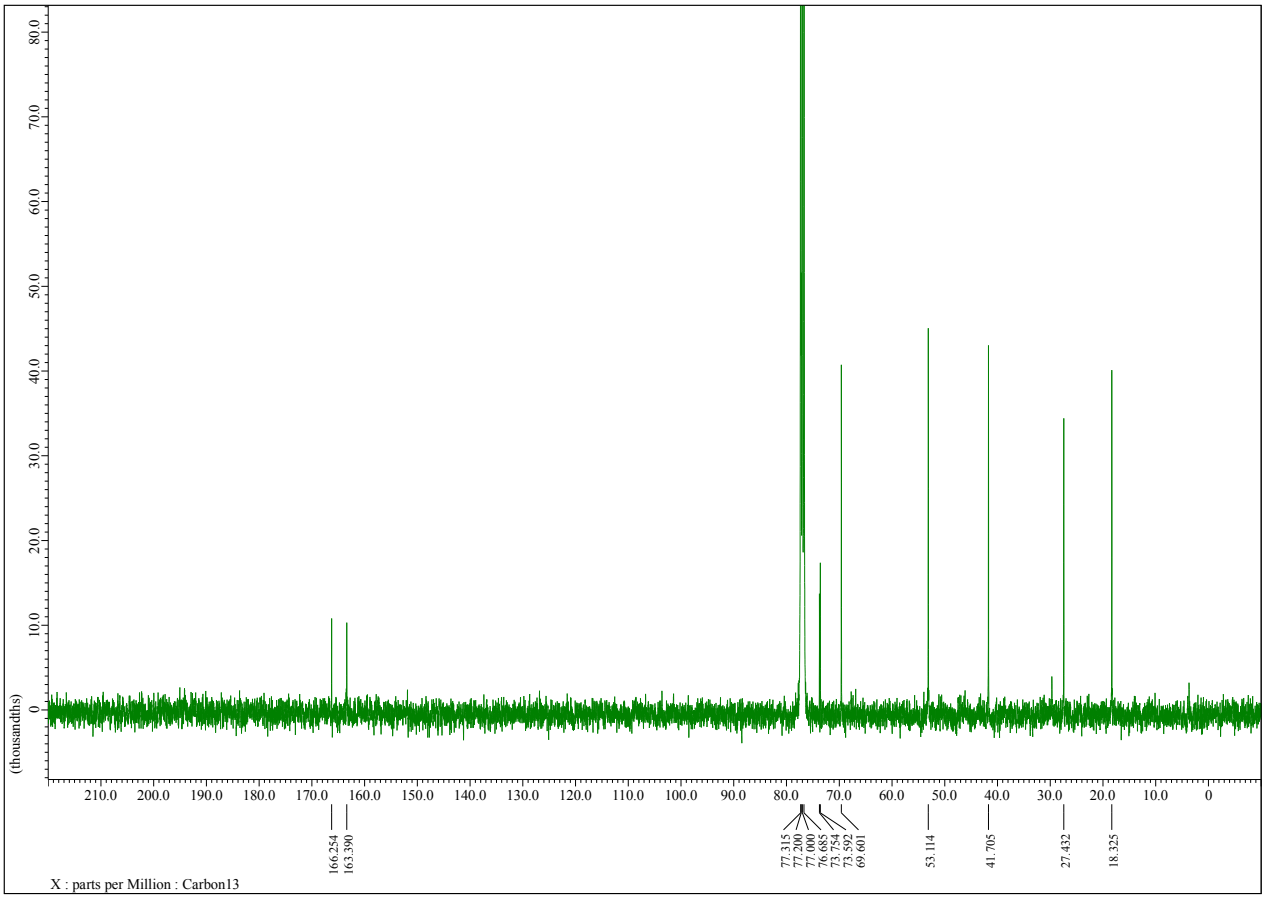
(thousandths)
X : parts per Million : Carbon13
166.254
163.390
77.315
77.200
77.000
76.685
73.754
73.592
69.601
53.114
41.705
27.432
18.325

***syn*-5b**

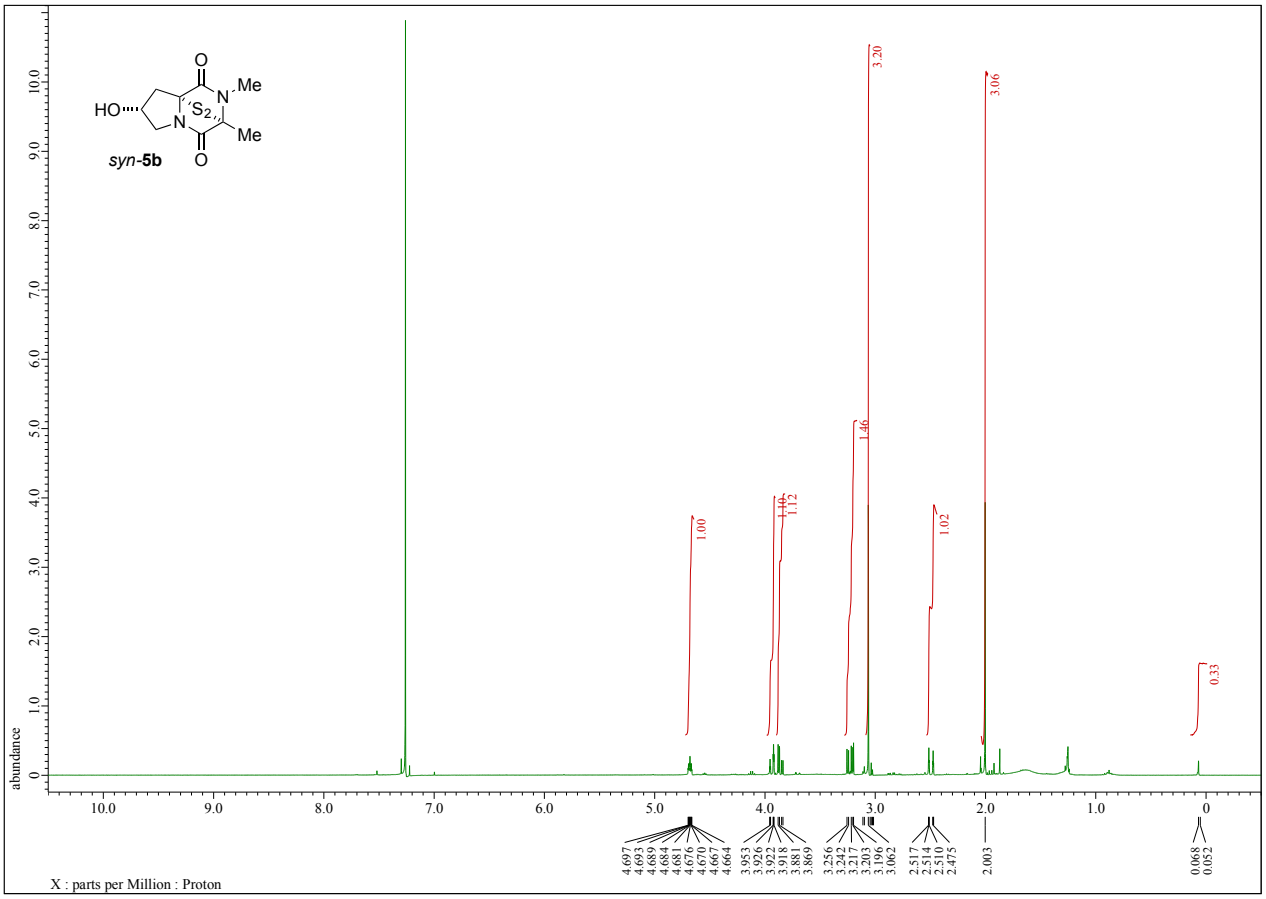
HO
O
N
Me
S2
N
Me
O
syn-5b
abundance
X : parts per Million : Proton
3.20
3.06
1.46
1.12
1.06
1.00
1.02
0.33

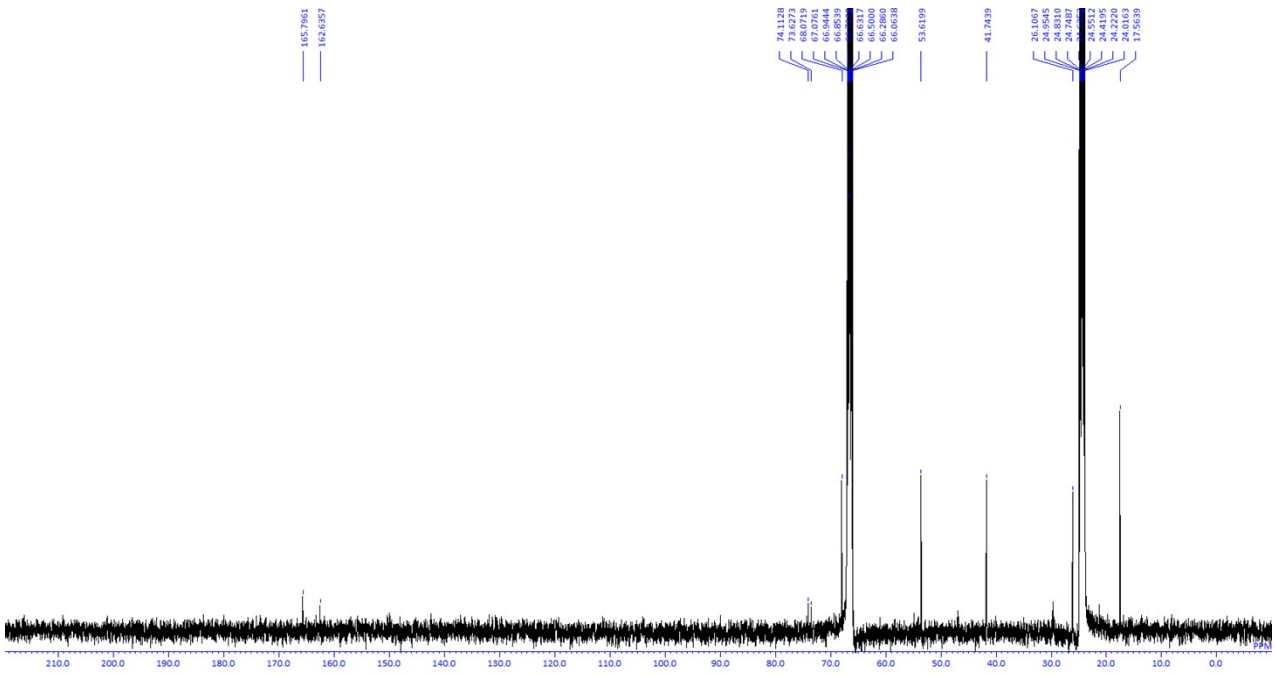
165.7961
162.6357
74.1128
73.6273
68.0719
67.6761
66.6844
66.6558
66.6317
66.5000
66.2860
66.0658
53.6199
41.7439
26.1067
24.9545
24.8310
24.7487
24.4195
24.2220
24.0163
17.5639
PPM

(*S*)-Selenohomoocystine (**S6**)

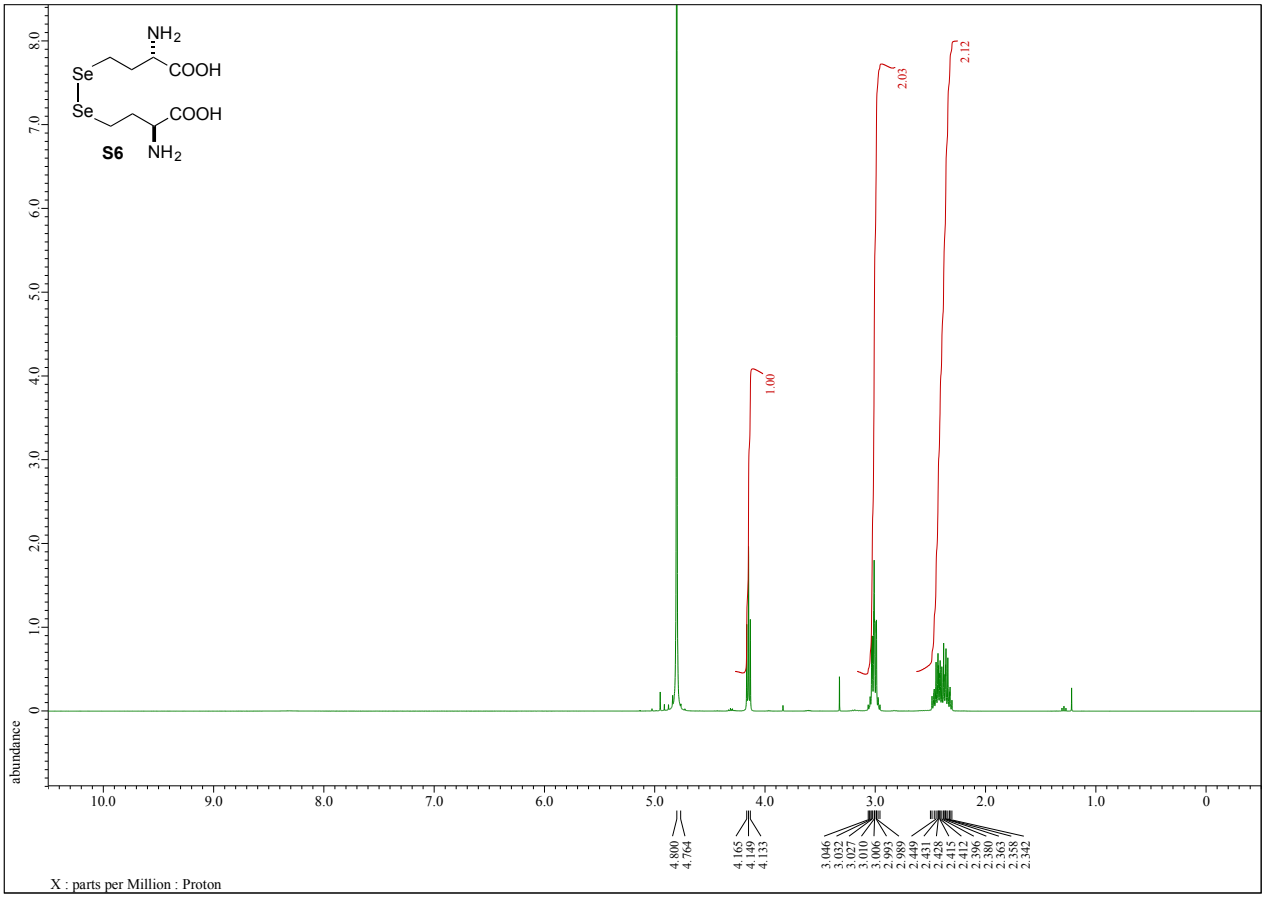

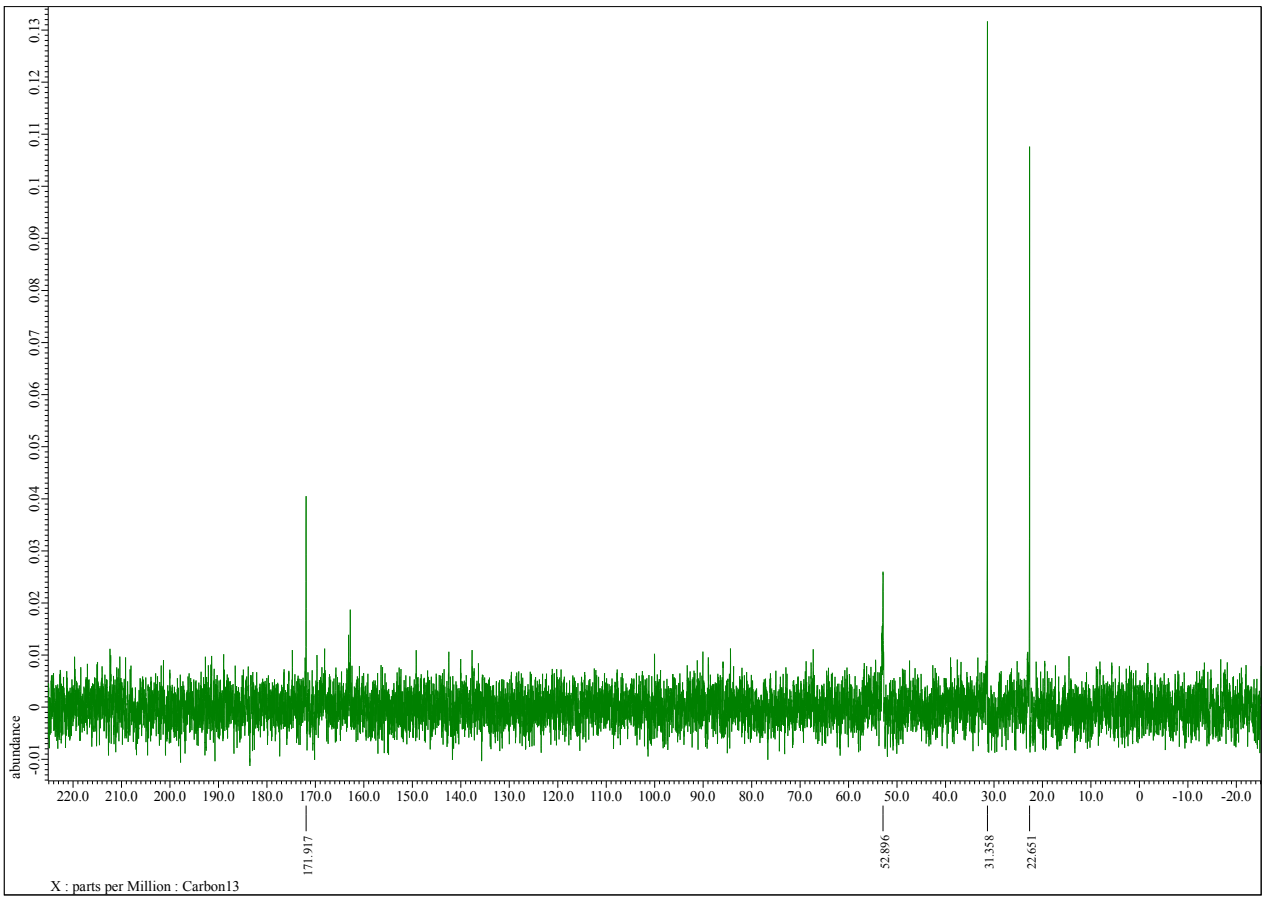

(*S*)-Se-adenosylselenohomocysteine (SeAH: **S7**)

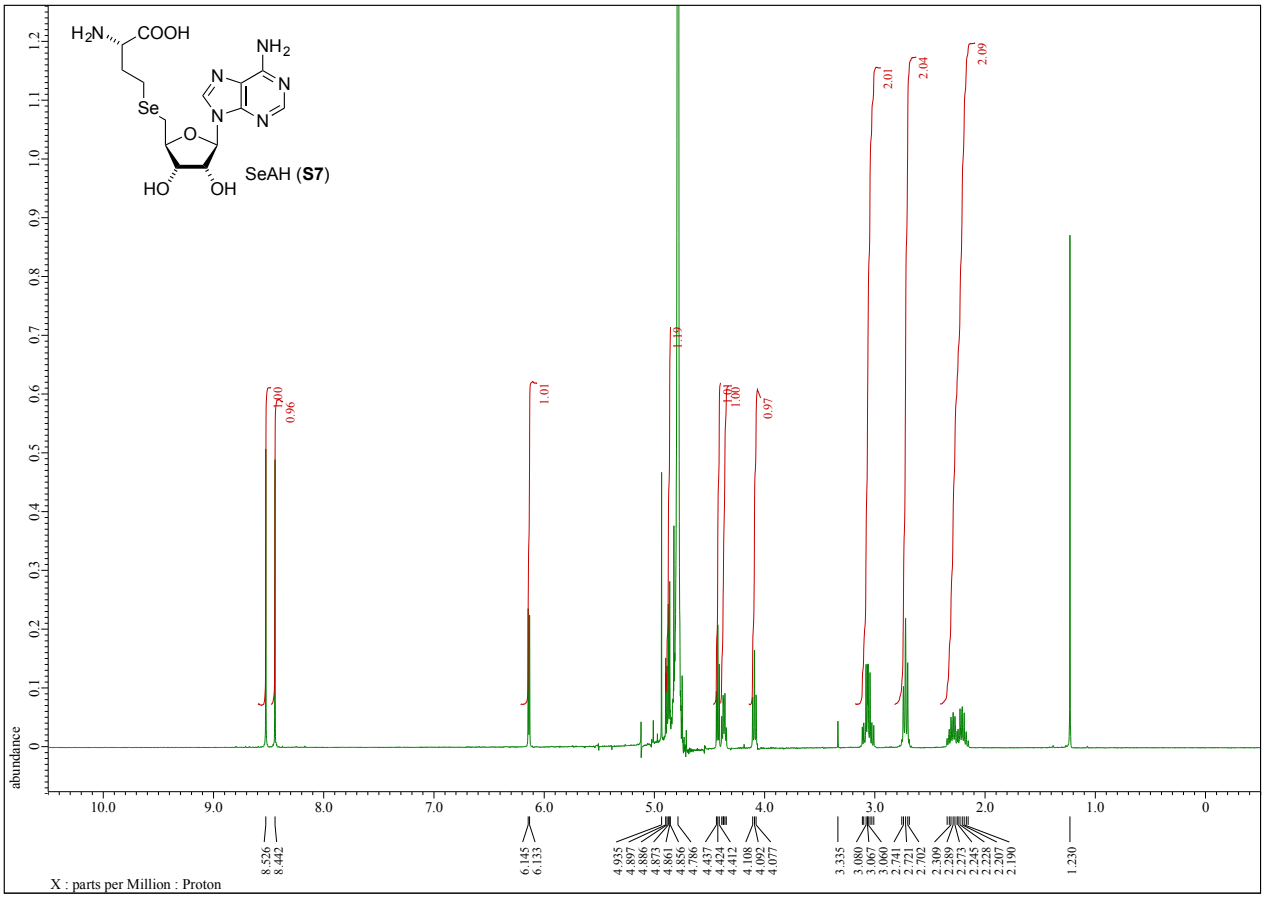

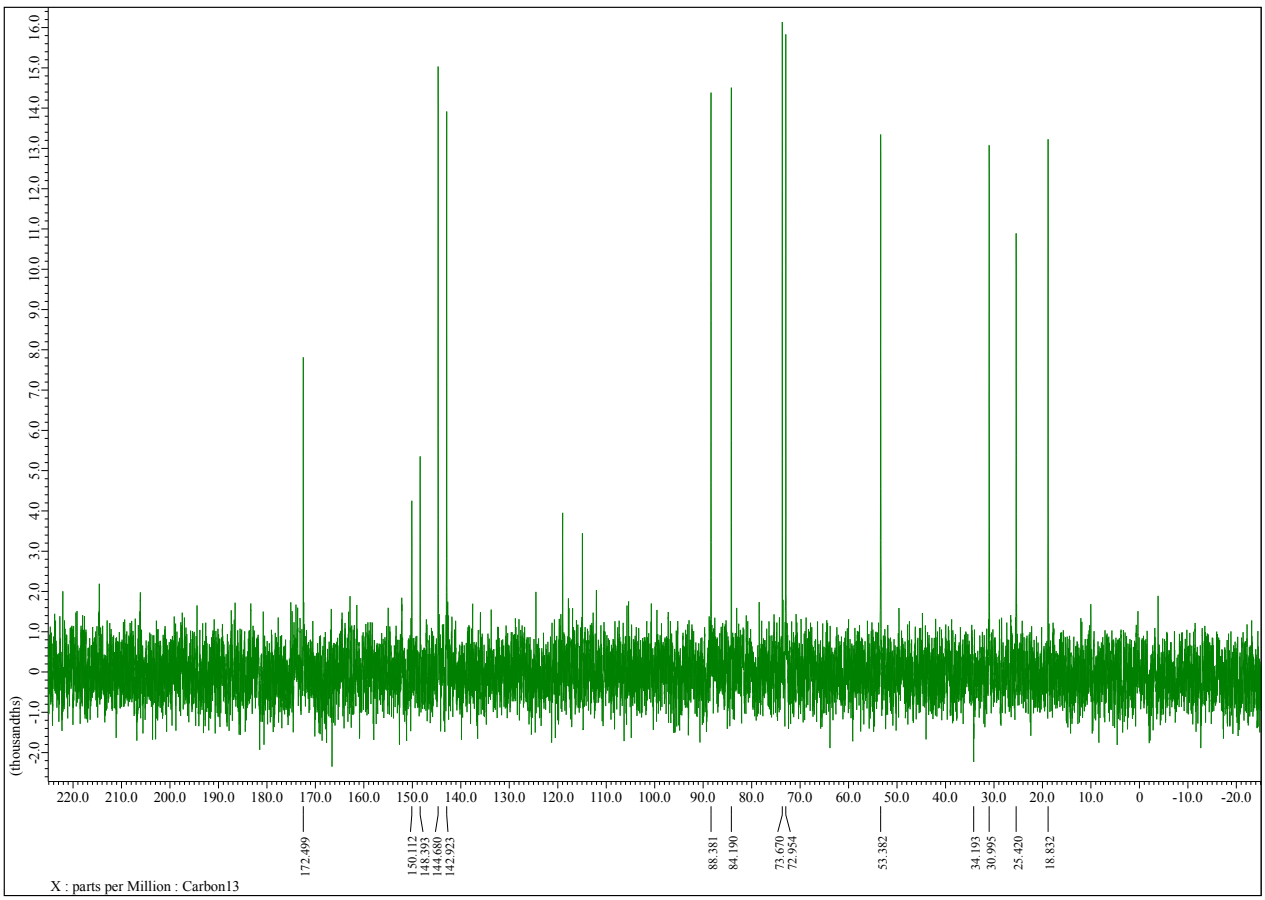

Propargylic Se-adenosyl-homocystein (ProSeAM: **1**)

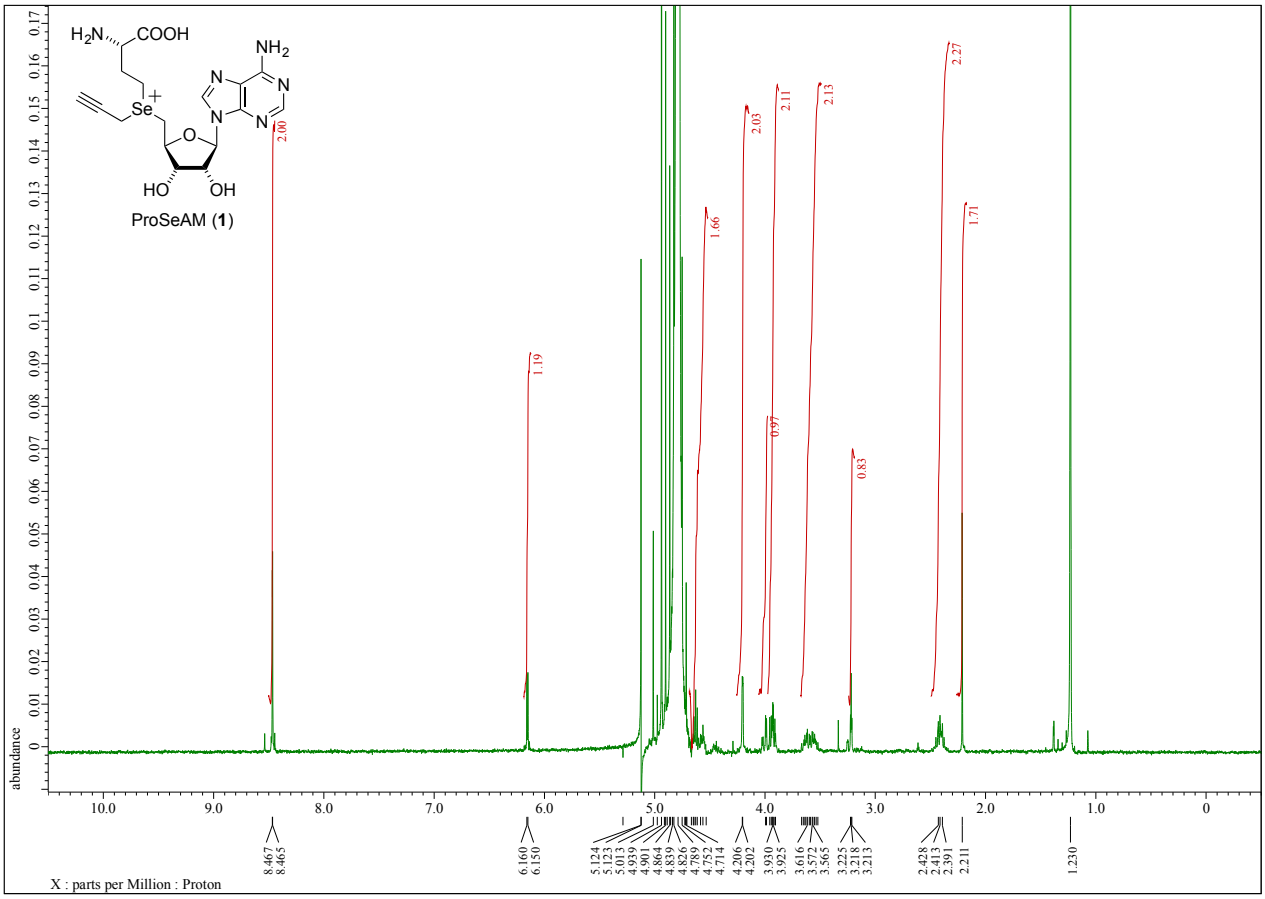

13. References

For full author information for ref 24 in the main text.

C. H. Arrowsmith, J. E. Audia, C. Austin, J. Baell, J. Bennett, J. Blagg, C. Bountra, P. E. Brennan, P. J. Brown, M. E. Bunnage, C. Buser-Doepner, R. M. Campbell, A. J. Carter, P. Cohen, R. A. Copeland, B. Cravatt, J. L. Dahlin, D. Dhanak, A. M. Edwards, M. Frederiksen, S. V. Frye, N. Gray, C. E. Grimshaw, D. Hepworth, T. Howe, K. V. M. Huber, J. Jin, S. Knapp, J. D. Kotz, R. G. Kruger, D. Lowe, M. M. Mader, B. Marsden, A. Mueller-Fahrnow, S. Müller, R. C. O'Hagan, J. P. Overington, D. R. Owen, S. H. Rosenberg, R. Ross, B. Roth, M. Schapira, S. L. Schreiber, B. Shoichet, M. Sundström, G. Superti-Furga, J. Taunton, L. Toledo-Sherman, C. Walpole, M. A. Walters, T. M. Willson, P. Workman, R. N. Young and W. J. Zuercher

[S1] S. Fujishiro, K. Dodo, E. Iwasa, Y. Teng, Y. Sohtome, Y. Hamashima, A. Ito, M. Yoshida and M. Sodeoka, *Bioorg. Med. Chem. Lett.,* 2013, **23**, 733–736.

[S2] E. Iwasa, Y. Hamashima, S. Fujishiro, E. Higuchi, A. Ito, M. Yoshida and M. Sodeoka, *J. Am. Chem. Soc*., 2010, **132**, 4078–4079.

[S3] E. Iwasa, Y. Hamashima, S. Fujishiro and M. Sodeoka, *Tetrahedron* 2011, **67**, 6587–6599.

[S4] E. Veverkova, L. Liptakova, M. Veverka and R. Sebesta, *Tetrahedron: Asymmetry*, 2013, **24**, 548–552.

[S5] K. C. Nicolaou, D. Giguère, S. Totokotsopoulos, and Y.-P, Sun, *Angew. Chem., Int. Ed*., 2012, **51**, 728–732.

[S6] K. C. Nicolaou, M. Lu, S. Totokotsopoulos, P. Heretsch, D, Giguère, Y.-P, Sun, D. Sarlah, T. H. Nguyen, I. C. Wolf, D. F. Smee, C. W. Day, S, Bopp and E. A. Winzeler, *J. Am. Chem. Soc*., 2012, **134**, 17320–17332.

[S7] I. R. Bothwell, K. Islam, Y. Chen, W. Zheng, G. Blum, H. Deng and M. Luo, *J. Am. Chem. Soc*., 2012, **134**, 14905–14912.

[S8] S. Willnow, M. Martin, B. Luscher, and E. Weinhold, *ChemBioChem,* 2012, **13**, 1167–1173.

[S9] I. R. Bothwell and M. Luo, *Org. Lett*., 2014, **16**, 3056–3059.

[S10] N. Gauthier, M. Caron, L. Pedro, M. Arcand, J. Blouin, A. Labonte, C. Normand, V. Paquet, A. Rodenbrock, M. Roy, N. Rouleau, L. Beaudet, J. Padros and R. Rodriguez-Suarez, *J. Biomol. Screening,* 2012, **17**, 49−58.

[S11] Y. Takemoto, A. Ito, H. Niwa, M. Okamura, T. Fujiwara, T. Hirano, N. Handa, T. Umehara, T. Sonoda, K. Ogawa, M. Tariq, N. Nishino, S. Dan, H. Kagechika, T. Yamori, S. Yokoyama and M. Yoshida, *J. Med. Chem.,* 2016, **59**, 3650–3660.